

Free space transmission lines in receiving antenna operation

Reuven Ianconescu*, Vladimir Vulfin†

†Shenkar College of Engineering and Design, Ramat Gan, Israel, riancon@gmail.com

*Ben-Gurion University of the Negev, Beer Sheva 84105, Israel, vlad2042@yahoo.com

Abstract—This work derives exact expressions for the voltage and current induced into a two conductors non isolated transmission lines by an incident plane wave. The methodology is to use the transmission line radiating properties to derive scattering matrices and make use of reciprocity to derive the response to the incident wave. The analysis is in the frequency domain and it considers transmission lines of any small electric cross section, incident by a plane wave from any incident direction and any polarisation. The analytic results are validated by successful comparison with ANSYS commercial software simulation results, and compatible with other published results.

Index Terms—electromagnetic theory, guided waves, electromagnetic interference

I. INTRODUCTION

This work calculates the voltage and differential current developed on an ideal two-conductors TEM transmission line (TL) of any small electric cross section, connected to passive (lumped) loads and hit by a monochromatic plane wave, as shown in Figure 1. We derive both amplitude and phase for

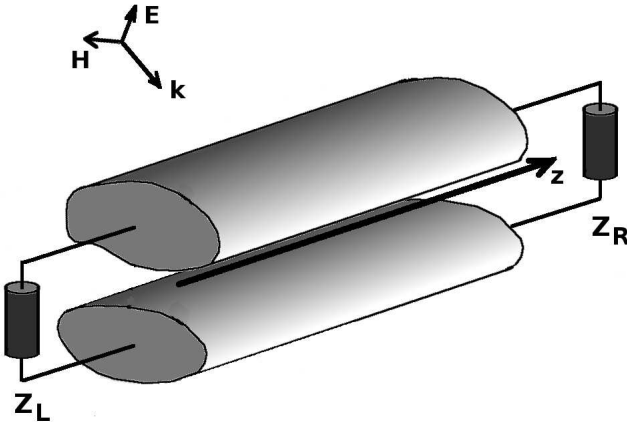


Fig. 1. Configuration of a two ideal conductors transmission line (TL), connected at both sides to passive loads: Z_L (left) and Z_R (right), hit by a monochromatic plane wave propagating toward the centre of coordinates. The cross section is electrically small and may be of any shape. The loads are located at the terminations of the TL, and are shown farther away, because of technical drawing limitations.

the voltage and current developed along the TL, and hence the powers delivered to the passive loads.

The configuration as defined here is a scattering problem, requiring a full wave solution to set the tangential component of the electric field to 0 on the surface of the TL. However,

we shall formulate here an analytic solution to this problem, which is compared with a full wave HFSS solution.

As shown in [1], the characteristic impedance Z_0 of the TL and an equivalent separation distance d can be found by an electrostatic cross section analysis, leading to a twin lead equivalent (examples for determining Z_0 and d are shown in Appendix B of [1]). The twin lead equivalent is shown in Figure 2. When the TL is excited at its port(s), this equivalent

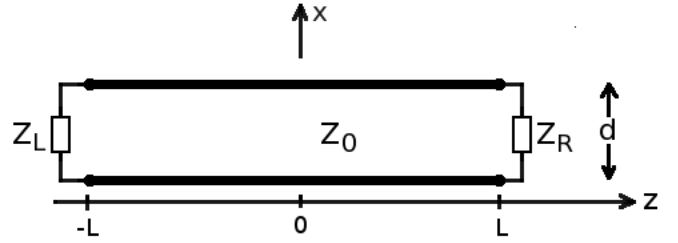


Fig. 2. Twin lead equivalent of the analysed transmission line, defined by the separation distance d between the conductors, and the characteristic impedance Z_0 , both computed by the cross section analysis described in Appendix B of [1]. The TL is of length $2L$.

twin lead radiates the same far fields as the actual TL. To emphasise, we *do not* solve for the twin lead geometry, but for an arbitrary cross section in Figure 1, the twin lead is only used as an intermediate tool for the calculations.

The incident plane wave shown in Figure 1 propagates toward the coordinates origin with phase $e^{-j\mathbf{k}\cdot\mathbf{r}}$, so that the wavenumber vector $\mathbf{k} = -\hat{\mathbf{r}}k$ points toward the origin. Expanding $\hat{\mathbf{r}}$ in Cartesian unit vectors, the phase can be written as

$$e^{jk[x \sin \theta \cos \varphi + y \sin \theta \sin \varphi + z \cos \theta]}, \quad (1)$$

where θ and φ are the spherical angles which represent the direction of the plane wave arrival.

The polarisation of the incident plane wave is shown in Figure 3. It travels toward the centre of coordinates, perpendicular to the θ, φ plane, with a polarisation angle α from the θ axis, so that the E field at the origin, where its phase is 0 (see Eq. (1)) is given by

$$\mathbf{E} = E_0(\hat{\boldsymbol{\theta}} \cos \alpha + \hat{\boldsymbol{\varphi}} \sin \alpha) \quad (2)$$

or its components

$$E_\theta = E_0 \cos \alpha \quad ; \quad E_\varphi = E_0 \sin \alpha. \quad (3)$$

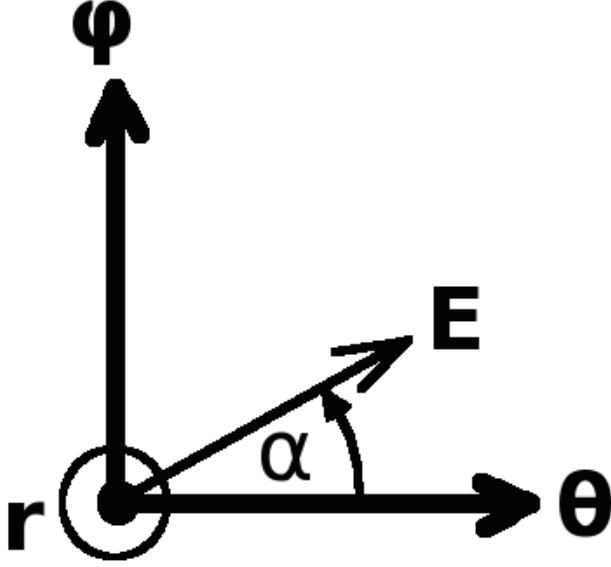


Fig. 3. The incident plane wave propagates toward the centre of coordinates in the $-\hat{r}$ direction. In spherical coordinates the local equiphase surface is θ, φ and the polarisation is at angle α from the θ axis, so that at the origin $\mathbf{E} = E_0(\hat{\theta} \cos \alpha + \hat{\varphi} \sin \alpha)$ (see Eq. (2)).

Such problem has been handled in [2]–[6], but not for an arbitrary cross section (as in Figure 1), and not for a general incident plane wave (as in Figure 3). The methodology used in these works is based on a generalisation of the telegraph equations for transmission lines, for the twin lead geometry indicated in Figure 2. Given C' and L' the capacitance and inductance per unit length, using $Z_0 = \sqrt{L'/C'}$ and the identity $\sqrt{L'C'} = 1/c$, we write the (inhomogeneous) telegraph equations in the following compact form

$$\frac{dV}{dz} + jk(Z_0 I) = V_s \quad (4)$$

$$Z_0 \frac{dI}{dz} + jkV = Z_0 I_s \quad (5)$$

where the source terms V_s and I_s are induced by H_y and E_x fields of the incident plane wave, integrated along the x axis of the twin lead (see Figure 2), as follows:

$$V_s = jk\eta_0 \int_0^d H_y(x, z) dx \simeq jk\eta_0 H_y(z) d \quad (6)$$

$$Z_0 I_s = -jk \int_0^d E_x(x, z) dx \simeq -jk E_x(z) d, \quad (7)$$

and $\eta_0 = 377\Omega$ is the free space impedance. The last (\simeq) parts of Eqs. (6) and (7) are consistent with our framework which is restricted to small electric cross section ($kd \ll 1$).

The coupled non-homogeneous differential equations (4) and (5) can be decoupled into two second order equations:

$$\frac{d^2 V}{dz^2} + k^2 V = \frac{dV_s}{dz} - jk(Z_0 I_s) \quad (8)$$

$$Z_0 \frac{d^2 I}{dz^2} + k^2 Z_0 I = Z_0 \frac{dI_s}{dz} - jkV_s \quad (9)$$

In [2] the authors wrote the general solution for those second order differential equations, subject to the termination conditions:

$$V(-L) = -Z_L I(-L) \quad ; \quad V(L) = Z_R I(L), \quad (10)$$

however they used in the expression for the sources the implicit assumption that the incident field has only a H_y component. In [3] this solution has been simplified, and in [4]–[6] this formalism has been extended to multiconductor TL.

The results derived in this work satisfy Eqs. (4)–(10), but we use a different technique to derive them. We shall use our knowledge on the radiation properties of TL [1] to derive the receiving properties, i.e. the response of a TL to an incident monochromatic plane wave described in Figure 3. To determine the voltage along the TL, we segment it into M parallel ports as shown in Figure 4. The ports 1 and M are

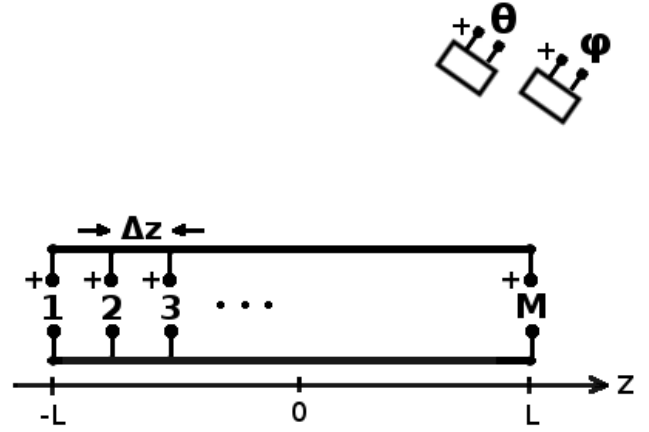


Fig. 4. M parallel ports along the TL, adjacent ports are at distance Δz . Ports 1 and M are defined for the TL impedance Z_0 , and the middle ports 2 .. $M - 1$ are defined for a high impedance Z_H . Two additional ports representing far antennas matched for the $\hat{\theta}$ and $\hat{\varphi}$ polarizations are defined. Those ports are named θ and φ , and are defined for the TL impedance Z_0 .

defined for the TL impedance Z_0 , and the middle ports 2 .. $M - 1$ are defined for a high impedance $Z_H \rightarrow \infty$. We define two additional ports representing far antennas matched for the $\hat{\theta}$ and $\hat{\varphi}$ polarizations of the field radiated by the TL, defining a system of $M + 2$ ports. The additional ports, $M + 1$ and $M + 2$, named θ and φ , may be defined for any impedance, and for convenience we choose to define them for the TL impedance Z_0 . The scattering matrix of this system is shown schematically in Figure 5. Using the formalism developed in [1], we know the $\hat{\theta}$ and $\hat{\varphi}$ components of the radiated electric field (summarised in Appendix A). Those field components are translated into voltages using a normalisation explained in Appendix A, enabling us to calculate the generalised S matrix (see Appendix B) describing this system.

Here we excite this system with an incident voltage, scaled to the incident electric field in Eq. (2) by

$$V^+ = E_0 d, \quad (11)$$

which defines the voltage components (equivalent to Eq. (3))

$$V_\theta^+ = V^+ \cos \alpha \quad ; \quad V_\varphi^+ = V^+ \sin \alpha. \quad (12)$$

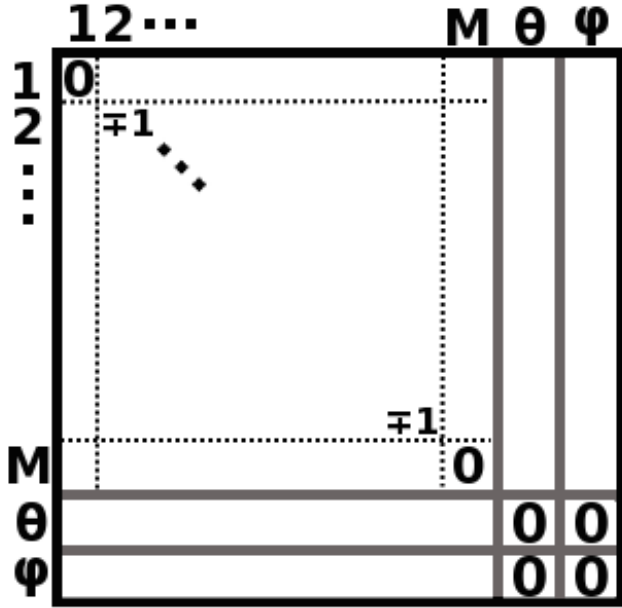


Fig. 5. Schematic diagram of a $(M + 2) \times (M + 2)$ scattering matrix describing the systems defined in Figures 4 and 6. The first ports 1.. M are the TL ports in the figures, and the two additional ports are the far θ or φ polarised antennas, named θ , φ . In both cases $S_{\theta\varphi} = S_{\varphi\theta} = 0$, because they are orthogonally polarised, and $S_{11} = S_{MM} = S_{\theta\theta} = S_{\varphi\varphi} = 0$. As will be shown, the elements S_{ii} for $1 < i < M$ are ∓ 1 for the matrices defined by the configurations in Figures 4 and 6, respectively.

We note that ports 1... M are matched with the Z_0 impedance at ports 1 and M and Z_H (i.e. infinite) on the middle ports, which is exactly the configuration of a TL matched at both terminations, on which we want to obtain the voltages.

Those are obtained by multiplying the S matrix by the column vector

$$\begin{pmatrix} 0 \\ \cdot \\ \cdot \\ \cdot \\ 0 \\ \frac{0}{V_{\theta}^+} \\ V_{\varphi}^+ \end{pmatrix} \quad (13)$$

of adequate excitation elements according to Eq. (12), and given Δz is arbitrarily small (or M arbitrarily large) we obtain the voltage as function of z along the matched TL for the given incident plane wave. The solution for matched TL is after that generalised for any terminations in Figure 1.

Similarly, the analytic solution for the current is obtained by segmenting the TL into M serial ports as shown in Figure 6. Ports 1 and M are defined for the TL impedance Z_0 , and the middle ports 2 .. $M - 1$ are defined for a tiny impedance $Z_T \rightarrow 0$. Here we define too the additional ports representing far antennas matched for the $\hat{\theta}$ and $\hat{\varphi}$ polarizations of the field radiated by the TL, obtaining a *different* system of $M+2$ ports.

For this system we also calculate a generalised S matrix, but defined for current waves (see Appendix B). Here the methodology is similar to the one explained for the voltages, the matched at both terminations TL result is obtained using

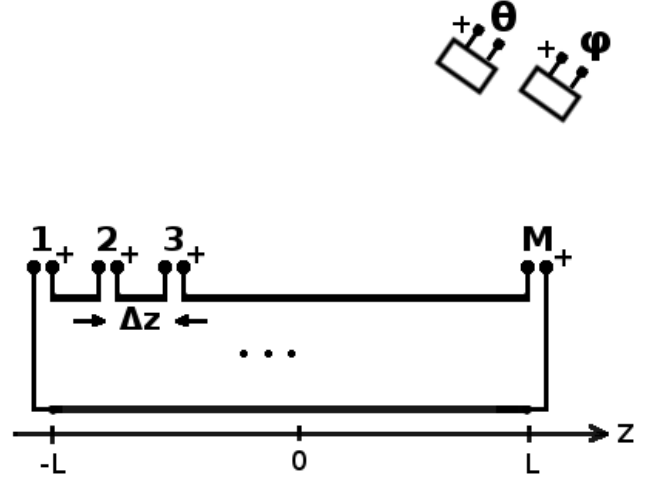


Fig. 6. M serial ports along the TL, adjacent ports are at distance Δz . Ports 1 and M are defined for the TL impedance Z_0 , and the middle ports 2 .. $M - 1$ are defined for a tiny impedance Z_T . The “+” is defined at the right side of the port, so that the port current is defined in the $+z$ direction. Note also that port 1 is physically identical to the one defined Figure 4 and so is port M , up to the sign. Here we define as well the two additional ports named θ and φ , defined for the TL impedance Z_0 .

Z_0 impedance at ports 1 and M and Z_T (i.e. 0) on the middle ports, so we first obtain the current on the matched TL and then generalise the result for any loads.

The advantages and novelties of our derivation are:

- The method of using the S matrix reciprocity to derive receiving characteristics from transmitting characteristics is original and may be extended to additional configurations.
- We do not limit ourselves to the twin lead cross section, presenting a general algorithm for TL of any small electric cross section.
- Our formulation is for a general incident plane wave, i.e. from an arbitrary direction θ , φ , and arbitrary polarisation α .
- The solution of Eqs. (8) and (9) in [2] subject to general termination conditions (10) is extremely complicated, and it is not obvious in this method how one first gets a simple solution for a matched at both terminations TL, and how to further generalise it. In our solution based on S parameters, this emerges naturally.

The work is organized as follows. In Section II we carry out all the analytic derivations for the voltage and differential current along a TL hit by a monochromatic plane wave. We start with the voltage on a TL with matched loads and generalise the result for a TL terminated in any loads (Z_L and Z_R , as in Figure 1). This derivation is technical but quite lengthy, therefore after deriving the voltage we give the final results for the current, which is calculated in Appendix C. Those calculations use the far E field radiated from segments of the TL (based on [1] and summarised in Appendix A) and the properties of the generalised scattering matrix summarised in Appendix B.

In Section III we describe the full wave HFSS simulations

performed, and explain some delicate issues regarding the measurements of voltage and current. To be mentioned that a TL hit by a monochromatic plane wave may develop common mode currents. However, our derivation of the current is based on the reciprocity of the system defined in Figure 6. The currents used to define the scattering matrix are differential, and for those differential currents we use the far fields developed in [1]. Hence, when we use the reciprocity to express the current developed on the TL as function of the plane wave excitation, we obtain only the differential part of the current, and this drawback applies also to the method used in [2]–[6]. If the purpose is to calculate the power on the loads, this is not a limitation, because the common mode does not affect this power, but this has to be taken into account in the current measurement in Section III.

In Section IV-A we validate the analytic results with full wave HFSS simulations for a cross section which is not a twin lead, showing that this formalism works for a general electrically small cross section. We compare the theoretical results obtained in Sections II for the voltage and differential current with full wave HFSS solutions for matched and non matched transmission lines. In Section IV-B we prove the analytical results obtained in Section II are fully compatible with the results obtained in [2]–[6] and therefore satisfy Eqs. (4)–(10).

In Section V we calculate general expressions for the powers transferred to the loads, and interpret them in terms of the transmission radiation patterns in [1] and incident plane wave polarisation. We show that the power in the “left” load is closely related to the transmitting properties of a source at the left termination and viceversa. In Section VI we show a full analysis of the connection between the radiation characteristics of TL calculated in [1] and the receiving characteristics calculated in this work.

The work is ended with some concluding remarks.

Note: through this work, the phasor amplitudes are RMS values, hence there is no 1/2 in the expressions for power. Also, it is worthwhile to mention that the results of this work depend on physical sizes relative to the wavelength, and hence are valid for all frequencies satisfying the condition of small electric cross section.

II. DERIVATION OF THE VOLTAGE AND DIFFERENTIAL CURRENT ALONG THE TL

We start with the voltages, analysing the system described in Figure 4.

As explained in the introduction, to find the voltages on a matched TL, i.e. for $Z_L = Z_R = Z_0$ in Figure 2, one needs only the cross elements between the group of ports 1... M and the group θ , φ of the S matrix.

However, to generalise the solution for the voltage along a TL loaded by and Z_L and Z_R , one needs additional elements of the S matrix, we therefore calculate here all the elements of the matrix for the system defined in Figure 4, schematically shown in Figure 5. This matrix satisfies

$$\mathbf{V}^- = \mathbf{S}\mathbf{V}^+, \quad (14)$$

where \mathbf{S} is an $(M+2) \times (M+2)$ matrix and \mathbf{V}^+ , \mathbf{V}^- are column vectors of incoming and outgoing voltages, respectively.

We start with the submatrix with indices 1 to M . Feeding a *middle* port $1 < n < M$, located at

$$z_n = -L + (n-1)\Delta z, \quad (15)$$

where

$$\Delta z = \frac{2L}{M-1} \quad (16)$$

with a forward (entering) voltage V_n^+ and terminating the other TL ports $1 \leq i \leq M$ by the impedances defined for those ports (i.e. Z_0 for ports 1 and M , and Z_H for the middle ports) results in a forward wave from $z = z_n$ to $z = L$ and a backward wave from $z = z_n$ to $z = -L$, because the waves encounter at the intermediate ports a very high impedance $Z_H \rightarrow \infty$.

The impedance seen at port n is $Z_0/2$, so the reflection coefficient is $S_{n,n} = \frac{Z_0/2 - Z_H}{Z_0/2 + Z_H} \simeq -1 + \frac{Z_0}{Z_H}$, therefore the port voltage is $V_n = V_n^+(1 + S_{n,n}) = V_n^+ Z_0/Z_H$. The outgoing voltages at ports $i \neq n$ are

$$V_{i \neq n}^- = V_n e^{-jk\Delta z|i-n|} = V_n^+ \frac{Z_0}{Z_H} e^{-jk\Delta z|i-n|}. \quad (17)$$

and for $i = n$

$$V_n^- = V_n^+ S_{n,n} = V_n^+ \left(-1 + \frac{Z_0}{Z_H} \right) \quad (18)$$

This results in the following (partial) n column of the S matrix

$$S_{1 \leq i \leq M, 1 < n < M} = \begin{cases} \frac{Z_0}{Z_H} e^{-jk\Delta z|i-n|} & i \neq n \\ -1 + \frac{Z_0}{Z_H} \simeq -1 & i = n \end{cases}, \quad (19)$$

see upper sign in Figure 5. For column $n = 1$ or M , the results are similar, only replace $\frac{Z_0}{Z_H}$ by 1, hence

$$S_{1 \leq i \leq M, n=1, M} = \begin{cases} e^{-jk\Delta z|i-n|} & i \neq n \\ 0 & i = n \end{cases} \quad (20)$$

Eqs. (19) and (20) define the upper left square of the S matrix, i.e. all the elements connecting the TL ports 1 to M - see Figure 5, on which the diagonal elements are shown, the upper sign relates to this system.

Now we add the columns $S_{\theta,n}$ and $S_{\varphi,n}$ (last columns in Figure 5), representing the far $\hat{\theta}$ and $\hat{\varphi}$ polarisation antennas, respectively.

Feeding a *middle* port $1 < n < M$ with the voltage V_n^+ and all other ports by their matched load, we calculate the far fields given in Eqs. (A.1)–(A.3), scaled to the voltages V_{θ}^- and V_{φ}^- according to Eq. (A.10).

We start with the contribution of the x currents given in Eqs. (A.1) and (A.2), see Figure 7. It is convenient to express the results using the distances from the feeding point to the terminations:

$$l_2 = L - z_n \quad ; \quad l_1 = z_n + L, \quad (21)$$

shown in Figure 7, where z_n is defined in Eq. (15). Hence in all following expressions, the value of n is “hidden” in l_1

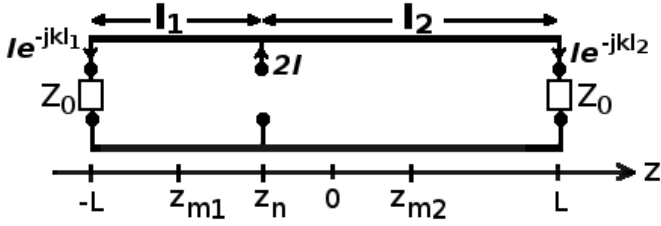


Fig. 7. Currents in the TL while feeding port n with V_n^+ . Defining $I \equiv V_n^+/Z_H$, the current in the feeding line at $z = z_n$ is $2I$ in the positive x direction, and the currents at $z = L$ (port M) and $z = -L$ (port 1) are Ie^{-jkl_2} and Ie^{-jkl_1} , respectively, both in the negative x direction. The z directed current waves are the forward wave in the region $[z_n, L]$ and the backward current wave in the region $[-L, z_n]$, to be used in Eq. (A.3). For the forward wave we use the current at the middle point $z_{m2} = (z_n + L)/2$, which is $Ie^{-jkl_2/2}$, while for the backward wave we use the current at $z_{m1} = (z_n - L)/2$: $-Ie^{-jkl_1/2}$ (minus because it flows in the $-z$ direction).

and l_2 . To shorten the notations in the forthcoming results we introduce two definitions

$$\begin{aligned} f_1 &\equiv e^{-jk(l_1+l_2 \cos \theta)/2} \sin(kl_1 \cos^2(\theta/2)) \\ f_2 &\equiv e^{-jk(l_2-l_1 \cos \theta)/2} \sin(kl_2 \sin^2(\theta/2)). \end{aligned} \quad (22)$$

Using Eqs.(A.1) for each of the three currents at $z_w = z_n, L$ and $-L$, scaling with (A.10), after some algebra we obtain:

$$V_{\theta}^-(x) = -jV_n^+(Z_0/Z_H)[f_1 + f_2] \cos \theta \cos \varphi \quad (23)$$

As evident from Eqs.(A.1) and (A.2), $V_{\varphi}^-(x)$ is identical to the above, up to replacing $\cos \theta \cos \varphi$ by $-\sin \varphi$, we therefore have

$$V_{\varphi}^-(x) = jV_n^+(Z_0/Z_H)[f_1 + f_2] \sin \varphi. \quad (24)$$

Next we calculate the contributions of the forward current wave in the region $z = [z_n, L]$ and the backward current wave in the region $z = [-L, z_n]$ (see Figure 7), using the upper and lower signs in Eq. (A.3), respectively. For the forward wave we use the current in the middle point $z_{m2} = (z_n + L)/2$, having the phase $e^{-jkl_2/2}$ for a TL length $h = l_2$, while for the backward wave we use the current at $z_{m1} = (z_n - L)/2$, having the phase $e^{-jkl_1/2}$, for a TL length $h = l_1$. Also the backward current is defined in the $-z$ direction, it therefore is taken with the minus sign. The middle points can be written more compactly as

$$z_{m2} = l_1/2 \quad ; \quad z_{m1} = -l_2/2, \quad (25)$$

and after scaling with (A.10), we obtain:

$$V_{\theta}^-(z) = 2jV_n^+(Z_0/Z_H) \cos \varphi [f_2 \cos^2(\theta/2) - f_1 \sin^2(\theta/2)] \quad (26)$$

Now we add the x and z directed currents contributions to $V_{\theta}^- = V_{\theta}^-(x) + V_{\theta}^-(z)$, using $1 - \cos(\theta) = 2 \sin^2(\theta/2)$ and $1 + \cos(\theta) = 2 \cos^2(\theta/2)$, after some algebra we obtain:

$$V_{\theta}^- = jV_n^+(Z_0/Z_H)[f_2 - f_1] \cos \varphi \quad (27)$$

V_{φ}^- has only the contribution of the x directed currents, given in Eq (24), hence

$$V_{\varphi}^- = V_{\varphi}^-(x). \quad (28)$$

Results (27) and (28) define the $S_{\theta,n}$ and $S_{\varphi,n}$ matrix elements respectively, for the columns $1 < n < M$:

$$S_{\theta, 1 < n < M} = j(Z_0/Z_H)[f_2 - f_1] \cos \varphi \quad (29)$$

$$S_{\varphi, 1 < n < M} = j(Z_0/Z_H)[f_1 + f_2] \sin \varphi. \quad (30)$$

For column $n = 1$ or M , the results are similar, only replace $\frac{Z_0}{Z_H}$ by 1, hence

$$S_{\theta, n=1, M} = j[f_2 - f_1] \cos \varphi \quad (31)$$

$$S_{\varphi, n=1, M} = j[f_1 + f_2] \sin \varphi. \quad (32)$$

The transpose elements are found by the reciprocity condition $S_{i,j}Z_j = S_{j,i}Z_i$ (see Appendix B, Eq. B.8), where Z_i and Z_j are the impedances for which ports i and j have been defined, respectively. Given the ports 1, M, θ and φ are defined for Z_0 of the TL and ports 2 .. $M-1$ are defined for Z_H , the transposed relations $S_{n,\theta}$ and $S_{n,\varphi}$ are given by Eqs. (31) and (32), for all n :

$$S_{n,\theta} = j[f_2 - f_1] \cos \varphi \quad (33)$$

$$S_{n,\varphi} = j[f_1 + f_2] \sin \varphi. \quad (34)$$

When issuing an excitation V_{θ}^+ from the θ port and matching all other ports, the voltages at ports n on the TL are $V_n^- = V_{\theta}^+ S_{n,\theta}$. Given the number M is not limited, one can get the continuous voltage on the TL for the excitation of the θ port:

$$V_{\theta}(z) = jV_{\theta}^+[f_2(z) - f_1(z)] \cos \varphi \quad (35)$$

where the z dependence in $f_{1,2}$ (see Eq. (22)) is in l_1 and l_2 , defined according to Eq. (21), using z for z_n . This voltage develops on the TL due to a $\hat{\theta}$ polarised plane wave coming from coordinates (θ, φ) at infinity.

Similarly for an excitation V_{φ}^+ from the φ port, while matching all other ports, one obtains the continuous voltage on the TL:

$$V_{\varphi}(z) = jV_{\varphi}^+[f_1(z) + f_2(z)] \sin \varphi. \quad (36)$$

which develops due to a $\hat{\varphi}$ polarised plane wave coming from coordinates (θ, φ) at infinity.

The total voltage developed on the matched TL is $V_{\theta}(z) + V_{\varphi}(z)$, where the intensities of V_{θ}^+ and V_{φ}^+ are according to Eq. (12). It comes out

$$V(z) = jV^+[f_2 \cos(\varphi - \alpha) - f_1 \cos(\varphi + \alpha)] \quad (37)$$

Eq. (37) is the final result for the voltage on a matched TL, i.e. terminated at both ends with resistors Z_0 . We now generalize the above result for a TL terminated with any loads at ports 1 and M : Z_L (left) and Z_R (right), respectively (see Figure 2). We express the generalized results in terms of the reflection coefficients:

$$\Gamma_L = \frac{Z_L - Z_0}{Z_L + Z_0} \quad \text{and} \quad \Gamma_R = \frac{Z_R - Z_0}{Z_R + Z_0}. \quad (38)$$

For the matched case, the only incoming voltage waves are V_{θ}^+ and V_{φ}^+ , while all other $V_{1 \leq i \leq M}^+ = 0$. Here we have two additional incoming voltages at the mismatched ports 1 and M :

$$V_1^+ = \Gamma_L V_1^- \quad \text{and} \quad V_M^+ = \Gamma_R V_M^-, \quad (39)$$

while at the matched (with Z_H) ports $n = 2..M - 1$ the incoming voltages are 0:

$$V_{2 \leq n \leq M-1}^+ = 0. \quad (40)$$

We use the general connection for $1 \leq n \leq M$ (i.e. on TL) but $1 \leq i \leq M + 2$, i.e. all excitations including θ and φ :

$$V_n^- = \sum_{i=1}^{M+2} S_{n,i} V_i^+ = S_{n,1} V_1^+ + S_{n,M} V_M^+ + V(z) = S_{n,1} \Gamma_L V_1^- + S_{n,M} \Gamma_R V_M^- + V(z) \quad (41)$$

where the only non zero terms are $i = 1, M, \theta$ and φ (see Eq (40)), and the last two terms $i = \theta, \varphi$ represent the matched voltage at $z = z_n$, given in (35), (36), summed in (37). In the last form of Eq. (41), we used (39).

For $n = 1$, Eq. (41) becomes

$$V_1^- = \Gamma_R V_M^- e^{-jk2L} + V(-L). \quad (42)$$

because $S_{1,1} = 0$, $S_{1,M} = S_{M,1} = e^{-jk2L}$ and $z_n = -L$.

For $n = M$, Eq. (41) reads

$$V_M^- = \Gamma_L V_1^- e^{-jk2L} + V(L). \quad (43)$$

because $S_{M,M} = 0$ and $z_n = L$.

Using $S_{n,1} = e^{-jkl_1}$, $S_{n,M} = e^{-jkl_2}$, for $2 \leq n \leq M - 1$, Eq. (41) becomes

$$V_{2 \leq n \leq M-1}^- = e^{-jkl_1} \Gamma_L V_1^- + e^{-jkl_2} \Gamma_R V_M^- + V(z), \quad (44)$$

where in principle $V(z)$ here excludes the terminations, but as we shall see this exclusion is not necessary. We solve now Eqs. (42) and (43) for V_1^- and V_M^- and obtain:

$$V_1^- = \frac{\Gamma_R e^{-j2kL} V(L) + V(-L)}{1 - \Gamma_L \Gamma_R e^{-j4kL}} \quad (45)$$

$$V_M^- = \frac{\Gamma_L e^{-j2kL} V(-L) + V(L)}{1 - \Gamma_L \Gamma_R e^{-j4kL}}. \quad (46)$$

To avoid confusions the generalised (non-matched) results are subindexed ‘‘NM’’. The total (non matched) voltage $V_{\text{NM}}(z_n) = V_n^+ + V_n^-$. For ports 1 or M, this voltage is

$$V_{\text{NM}}(-L) = V_1^-(1 + \Gamma_L) \quad (47)$$

$$V_{\text{NM}}(L) = V_M^-(1 + \Gamma_R). \quad (48)$$

For the ports $2 \leq n \leq M - 1$, $V_n^+ = 0$ (40), therefore Eq. (44) describes the total voltage on those ports. Taking the limit $z \rightarrow -L$ of Eq. (44), using (42) we find it reduces to (47) and similarly the limit $z \rightarrow L$ of Eq. (44) reduces to (48), therefore Eq. (44) describes the non matched voltage on the TL at all ports (in the continuum, for all z)

$$V_{\text{NM}}(z) = V(z) + \Delta V(z), \quad (49)$$

where $\Delta V(z)$ is the correction term due to non matching (first two terms in (44)):

$$\Delta V(z) = e^{-jkl_1} \Gamma_L V_1^- + e^{-jkl_2} \Gamma_R V_M^-, \quad (50)$$

and V_1^- and V_M^- are given in Eqs. (45) and (46).

This concludes the voltage developed on the TL due to a monochromatic plane wave, for a TL matched at both ends,

the solution is Eq. (37) and for general terminations we add the correction term in Eq. (50).

A similar calculation is carried out to find the differential current developed on the TL due to a monochromatic plane wave. This is done by analysing the system defined in Figure 6. Because this calculation is lengthy, and similar to this carried out on the system defined in Figure 4, it is done in Appendix C, and the results are given below.

The currents on a TL matched on both terminations due to θ or φ polarisations are:

$$I_\theta(z) = -j(V_\theta^+/Z_0)[f_1(z) + f_2(z)] \cos \varphi \quad (51)$$

$$I_\varphi(z) = j(V_\varphi^+/Z_0)[f_1(z) - f_2(z)] \sin \varphi, \quad (52)$$

and the total current for matched TL is their sum:

$$I(z) = -j(V^+/Z_0)[f_1 \cos(\varphi + \alpha) + f_2 \cos(\varphi - \alpha)] \quad (53)$$

It is easy to check that Eqs. (37) and (53) satisfy the termination conditions (10) with $Z_L = Z_R = Z_0$.

For a TL terminated in any impedances Z_L, Z_R , the differential current along the TL, I_{NM} (i.e. non matched) is

$$I_{\text{NM}}(z) = I(z) + \Delta I(z), \quad (54)$$

where $\Delta I(z)$ is the correction term due to non matching:

$$\Delta I(z) = -e^{-jkl_1} \Gamma_L I_1^- - e^{-jkl_2} \Gamma_R I_M^-, \quad (55)$$

and I_1^- and I_M^- are given explicitly in Eqs. (C.26) and (C.27), and also satisfy

$$V_1^- = -Z_0 I_1^- \quad ; \quad V_M^- = Z_0 I_M^- \quad (56)$$

The solutions (49) and (54) satisfy the termination conditions (10).

III. FULL WAVE HFSS SIMULATIONS

We describe in this Section the HFSS simulations done for the scattering problem defined in Figure 1. The results of this simulations are compared in the next section with the analytic results. We used a non twin lead cross section (used also in [1]), shown in Figure 8. For this cross section one knows analytically the distance d in the twin lead representation (shown as red points in Figure 8) by image theory, yielding

$$d = \sqrt{s^2 - (2a)^2} = 2.537\text{cm}, \quad (57)$$

and also the characteristic impedance

$$Z_0 = \frac{\eta_0}{\pi} \ln \left(\frac{d+s}{2a} \right) = 105.6 \Omega \quad (58)$$

while for other cross sections those can be determined by an electrostatic ANSYS 2D Maxwell simulation, as shown in Appendix B of [1].

The electric field of a plane wave is by default $E_0 = 1\text{V/m}$ in the HFSS simulation, so to normalise the results for $E_0 d = 1\text{V}$ we divide the measured results by the value of d in Eq. (57).

For convenience, we shall use a fixed TL length of $l \equiv 2L = 125\text{cm}$, and test for different frequencies. We measure the voltage and current along the TL from $z = -61.25\text{cm}$ to

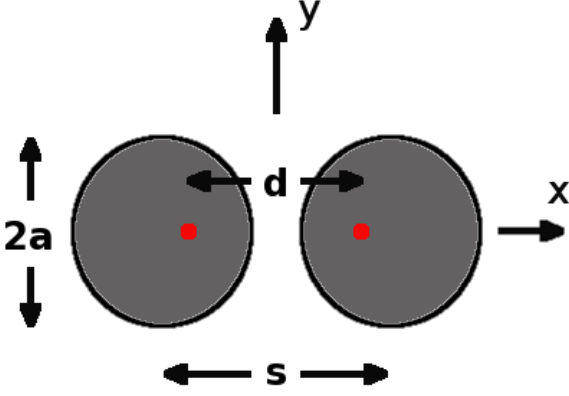


Fig. 8. Cross section of two parallel cylinders: the distance between the centres is $s = 3.59\text{cm}$, and the diameters are $2a = 2.54\text{cm}$. The red points show the current images which define the twin lead representation, and the distance between them $d = 2.537\text{cm}$ is calculated in Eq. (57).

$z = 61.25\text{cm}$ at intervals of 6.125cm , in total at 21 points. At the TL terminations $z = -L$ and $z = L$, we use inactive lumped ports defined for the impedance we need at those terminations.

Two-conductors transmission lines excited *only* at terminations, develop the TEM mode, so that both E_z and H_z are 0. In such case one can measure the voltage by $\int \mathbf{E} \cdot d\mathbf{l}$ from the “+” to the “-” conductor and the current using $\oint \mathbf{H} \cdot d\mathbf{l}$ around the “+” conductor, both on *any* integration path.

In the case analyzed here, the TL is excited by an external plane wave, therefore, depending on the incidence of this wave E_z and/or H_z are not necessarily 0, we therefore need more careful definitions for the voltage and current measurements, as described in the following subsections.

A. Voltage measurement

The voltage measured by the integral $\int \mathbf{E} \cdot d\mathbf{l}$ in the cross section depends on the chosen integration path if $H_z \neq 0$, as shown in Figure 9. To define the correct path we look at the definitions of the parallel ports in Figure 4. Those have been defined on the $x-z$ plane, so that *only* x directed currents flow through the port, and this fact has been used in the calculation of the S matrix in Section II, see Figure 7.

Therefore, to be consistent with the parallel ports definition, the correct path to measure the voltage is path A (on the x axis) shown in Figure 9, and this path is used in all the voltage measurements in Section IV.

B. Current measurement

For the case $E_z = 0$, the current can be measured by $\oint \mathbf{H} \cdot d\mathbf{l}$ around the “positive” conductor, on any integration path, like path C in Figure 10. In the opposite case consisting in an incident plane wave for which $E_z \neq 0$ (as shown in the figure), not only the integration path has to be tight around the conductor, but also, due to common mode current, one has to

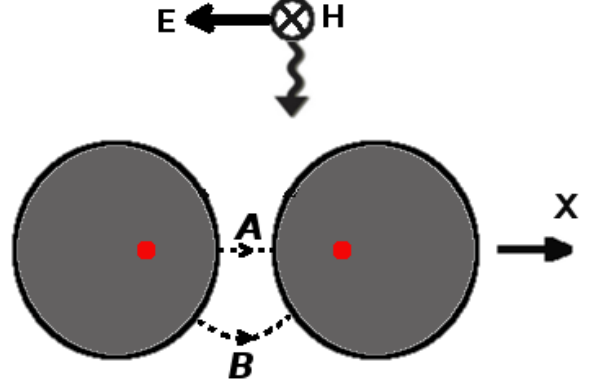


Fig. 9. Cross section voltage measurement on two possible paths A and B. In case $H_z = 0$, all paths lead to the same result, namely $\int_A \mathbf{E} \cdot d\mathbf{l} = \int_B \mathbf{E} \cdot d\mathbf{l}$. However, if $H_z \neq 0$, as for the incident plane wave shown here, the result of the path integral depends on the paths used, and the correct voltage measurement is $\int_A \mathbf{E} \cdot d\mathbf{l}$, i.e. along the x axis consistent with the parallel ports definition in Figure 4.

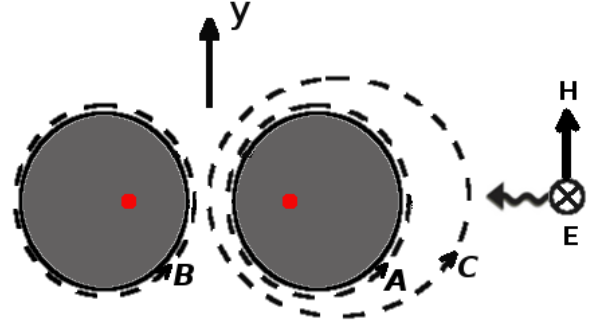


Fig. 10. Cross section differential current measurement for the case $H_z \neq 0$ requires integration on tight loops around each conductor from which one obtains the currents I_A and I_B (Eq. (59)). The differential current is calculated in Eq. (60).

measure around both conductors, on paths A and B, as shown in Figure 10, to obtain the currents

$$I_A = \oint_A \mathbf{H} \cdot d\mathbf{l} \quad ; \quad I_B = \oint_B \mathbf{H} \cdot d\mathbf{l}. \quad (59)$$

As one notes from the derivation in Section C, the S matrix has been derived from differential currents, so the analytic results (51) and (52) represent differential currents. To compare the HFSS simulation results to the analytic results we calculate the simulation differential current:

$$I = (I_A - I_B)/2; \quad (60)$$

If $H_z = 0$, I_B trivially reduces to $-I_A$, so that the differential current is the current on the “positive” conductor, which may be calculated by integrating on any path around it, like paths A or C in Figure 10.

IV. VALIDATION OF THE ANALYTIC RESULTS

A. Comparisons with HFSS full wave solution

1) *Matched transmission line:* We validate in this section the analytic results for matched TL in Eqs (37) and (53)

by comparison with full wave solution of ANSYS HFSS simulation results, described in the previous section.

We analyse three examples, each from a main incidence direction, by plane waves traveling along the x , y or z axes. In all examples the incident electric field intensity satisfies $Ed = \eta_0 Hd = 1V$. The half length of the TL is $L = 0.625$ m (or the length $2L = 1.25$ m).

In the first example we examine a plane wave traveling from $\theta = \pi$, along the z axis, colinear with the TL, having the phase e^{-jkz} , as shown in Figure 11. For $\theta = \pi$, Eqs. (37) and (53)

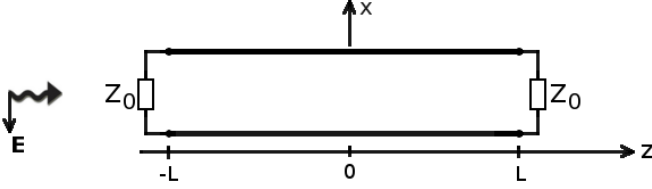


Fig. 11. Matched TL illuminated by a $-\hat{x}$ polarised plane wave from $\theta = \pi$.

(normalized by Z_0) reduce to

$$V(z) = V^+ j e^{-jkL} \sin[k(L-z)] \cos(\varphi - \alpha) \quad (61)$$

$$Z_0 I(z) = -V^+ j e^{-jkL} \sin[k(L-z)] \cos(\varphi - \alpha), \quad (62)$$

Clearly, at $\theta = \pi$, the angle φ is ill defined and so is the polarisation angle α (Figure 3), but the difference $\varphi - \alpha$ is meaningful. The maximum voltage and current occur at $\alpha = \varphi$ or $\pi - \varphi$, representing two opposite polarisations. Choosing $\alpha = \varphi$ the polarisation in Figure 3 becomes $\hat{\theta} \cos \varphi + \hat{\varphi} \sin \varphi$, which equals $-\hat{x}$ as shown in Figure 11 and using $V^+ = 1V$ Eqs. (61) and (62) become

$$V(z) = j e^{-jkL} \sin[k(L-z)] \quad (63)$$

$$Z_0 I(z) = -j e^{-jkL} \sin[k(L-z)], \quad (64)$$

which behave oscillatory according to the frequency, with 0 value at right termination at $z = L$. We remark that for this plane wave $E_z = H_z = 0$ therefore the voltage and current can be measured on any paths (see Figures 9 and 10).

Figures 12-14 show the voltage and normalized current for the $-\hat{x}$ polarised plane wave from $\theta = \pi$ in Figure 11 for frequencies 30, 60 and 120MHz, or $L/\lambda = 1/16$, $1/8$ and $1/4$, respectively. The voltage at the left termination at $z = -L$ is $V(-L) = j e^{-jkL} \sin(2kL)$, resulting in $0.27 + j0.65$, $(1 + j)/\sqrt{2}$ and 0 for the cases $L/\lambda = 1/16$, $1/8$ and $1/4$, respectively. The normalized currents $Z_0 I(-L)$ gets the minus of the above values, satisfying the termination condition $V(-L) = -Z_0 I(-L)$.

In the next example we use a plane wave hitting from $\theta = \varphi = \pi/2$ with phase e^{jkz} as shown in Figure 15. For this direction Eqs. (37) and (53) (normalized by Z_0) reduce to

$$V(z) = V^+ \sin \alpha [1 - e^{-jkL} \cos(kz)] \quad (65)$$

$$Z_0 I(z) = j V^+ \sin \alpha e^{-jkL} \sin(kz), \quad (66)$$

The maximum is for $\alpha = \pm\pi/2$, so using $\alpha = \pi/2$, results according to Figure 3 in a $\hat{\varphi}$ polarisation which is $-\hat{x}$ at $\theta = \varphi = \pi/2$, as shown in Figure 15. We note that this is the

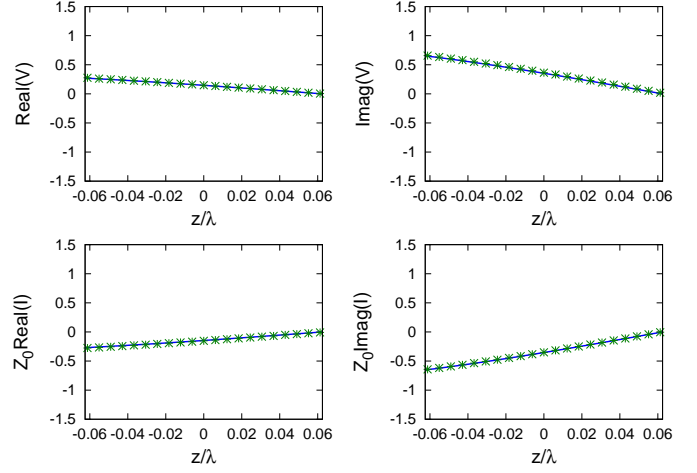


Fig. 12. Real and imaginary parts of the voltage $V(z)$ and normalized current $Z_0 I(z)$ for the plane wave incidence shown in Figure 11, at frequency 30MHz or $L/\lambda = 1/16$. The continuous line is the analytic solution in Eqs. (63) and (64) and the stars are the ANSYS simulation results.

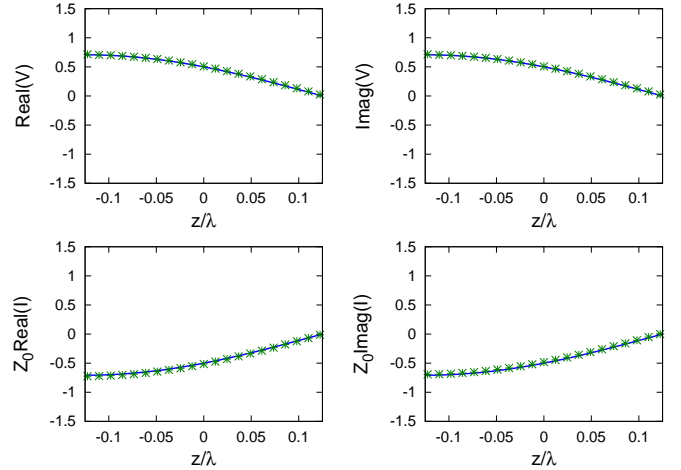


Fig. 13. Same as Figure 12, for frequency 60MHz or $L/\lambda = 1/8$.

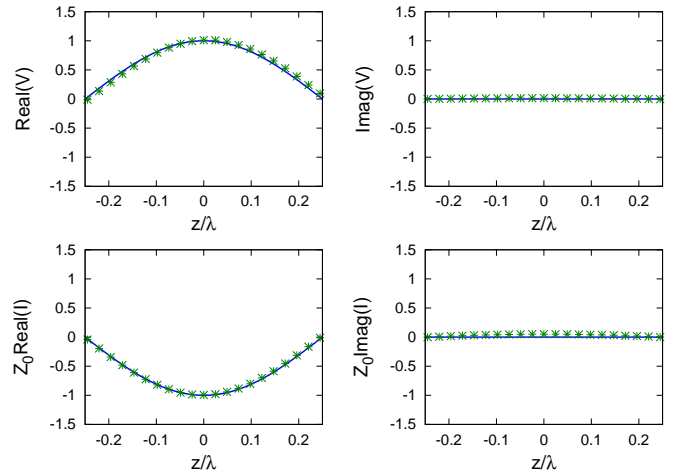


Fig. 14. Same as Figure 12, for frequency 120MHz or $L/\lambda = 1/4$.

same plane wave shown in Figure 9, so that here the path on

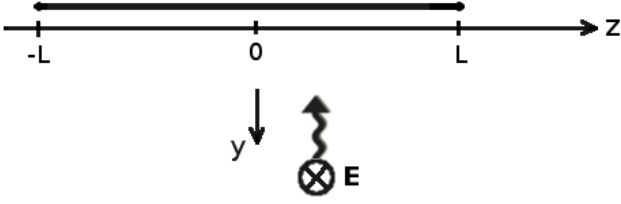


Fig. 15. Matched TL illuminated by a $-\hat{x}$ polarised plane wave from $(\theta = \pi/2, \varphi = \pi/2)$ (as also shown in Figure 9). The view is from the positive x axis direction, so that only the “upper positive” conductor is seen.

which one measures the voltage matters and must be path A in Figure 9.

Using $V^+ = 1V$ and $\alpha = \pi/2$ in Eqs. (65) and (66) result in

$$V(z) = 1 - e^{-jkL} \cos(kz) \quad (67)$$

$$Z_0 I(z) = j e^{-jkL} \sin(kz), \quad (68)$$

Figures 16-18 show the voltage and normalized current for the $-\hat{x}$ polarised plane wave from $\theta = \pi/2$ and $\varphi = \pi/2$ in Figure 11 for frequencies 30, 60 and 120MHz, or $L/\lambda = 1/16$, $1/8$ and $1/4$, respectively.

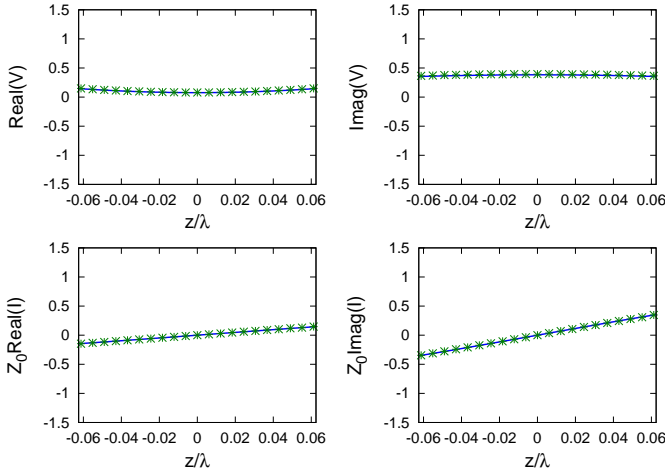


Fig. 16. Real and imaginary parts of the voltage $V(z)$ and normalized current $Z_0 I(z)$ for the plane wave incidence shown in Figure 15, at frequency 30MHz or $L/\lambda = 1/16$. The continuous line is the analytic solution in Eqs. (67) and (68) and the stars are the ANSYS simulation results.

As expected, the voltage is an even function of z and the current an odd function of z . Specifically, the voltages at the terminations at $z = -L$ and L are $0.146 + j0.354$, $0.5 + j0.5$ and 1 for the cases $L/\lambda = 1/16$, $1/8$ and $1/4$, respectively. The normalized currents have the same values at $z = L$, satisfying the termination condition $V(L) = Z_0 I(L)$, and minus the above values at $z = -L$, satisfying $V(-L) = -Z_0 I(-L)$.

The voltage in the middle of the TL at $z = 0$ are $0.076 + j0.383$, $1 - 1/\sqrt{2} + j/\sqrt{2}$ and $1 + j$ for the cases $L/\lambda = 1/16$, $1/8$ and $1/4$, respectively, and the current at $z = 0$ is of course 0.

In the next example we use a plane wave incident from $\theta = \pi/2$ and $\varphi = 0$, with phase e^{jkx} as shown in Figure 19.

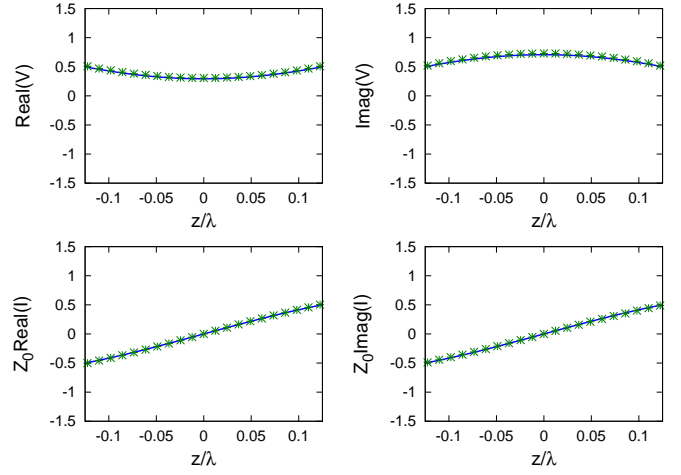


Fig. 17. Same as Figure 16, for frequency 60MHz or $L/\lambda = 1/8$.

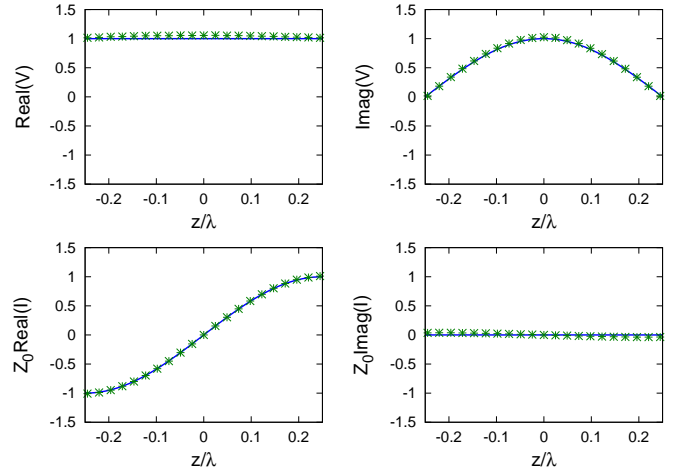


Fig. 18. Same as Figure 16, for frequency 120MHz or $L/\lambda = 1/4$.

For this direction Eqs. (37) and (53) (normalized by Z_0) reduce to

$$V(z) = -jV^+ \cos \alpha e^{-jkL} \sin(kz) \quad (69)$$

$$Z_0 I(z) = -V^+ \cos \alpha [1 - e^{-jkL} \cos(kz)]. \quad (70)$$

Here the maximum is obtained for $\alpha = 0$ or π . Using $\alpha = \pi$ defines according to Figure 3 a $-\hat{\theta}$ polarisation which equals \hat{z} at $\theta = \pi/2$ and $\varphi = 0$, as shown in Figure 19. This is the same plane wave mentioned in Figure 10, which requires current measurement by integrating on the tight trajectories A and B in Figure 10, using Eq. (60) to determine the differential current.

Using $V^+ = 1V$ and $\alpha = \pi$ in Eqs. (65) and (66) result in

$$V(z) = j e^{-jkL} \sin(kz) \quad (71)$$

$$Z_0 I(z) = 1 - e^{-jkL} \cos(kz), \quad (72)$$

Figures 20-22 show the voltage and normalized current for the \hat{z} polarised plane wave from $\theta = \pi/2$ and $\varphi = 0$ in Figure 19 for frequencies 30, 60 and 120MHz, or $L/\lambda = 1/16$, $1/8$ and $1/4$, respectively.

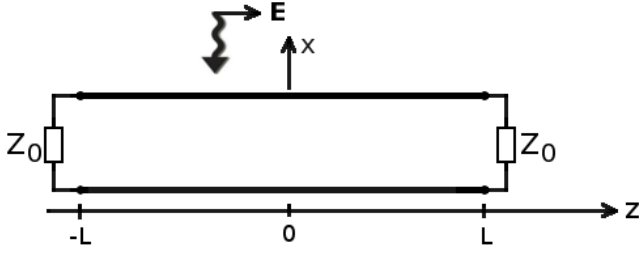


Fig. 19. Matched TL illuminated by a \hat{z} polarised plane wave from $(\theta = \pi/2, \varphi = 0)$ (as also shown in Figure 10).

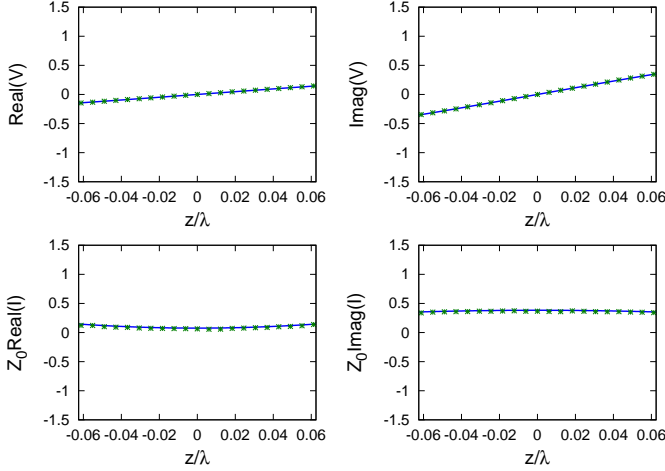


Fig. 20. Real and imaginary parts of the voltage $V(z)$ and normalized current $Z_0 I(z)$ for the plane wave incidence shown in Figure 19, at frequency 30MHz or $L/\lambda = 1/16$. The continuous line is the analytic solution in Eqs. (71) and (72) and the stars are the ANSYS simulation results.

As expected, the voltage is an odd function of z and the current an even function of z . The voltage developed for the incident field in Figure 19 (Eq. 71) has the value of the normalized current developed for the incident field in Figure 15 (Eq. 68) and viceversa.

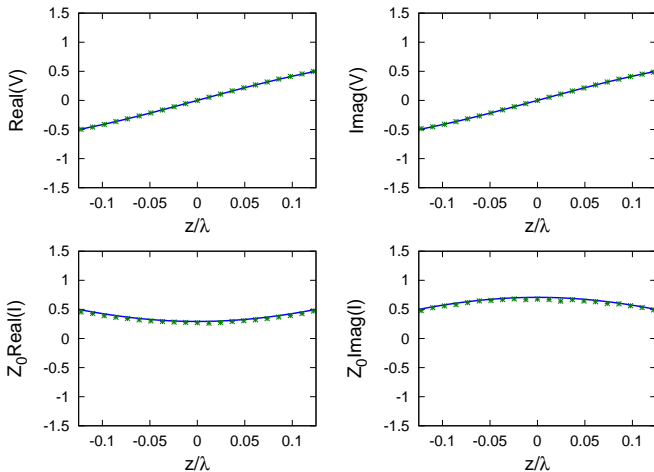


Fig. 21. Same as Figure 20, for frequency 60MHz or $L/\lambda = 1/8$.

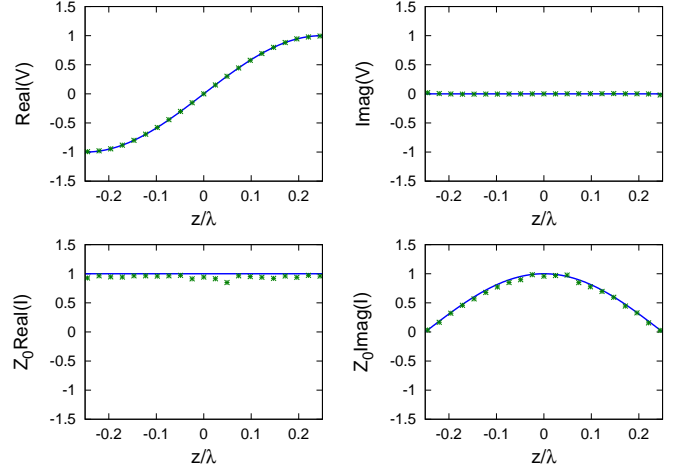


Fig. 22. Same as Figure 20, for frequency 120MHz or $L/\lambda = 1/4$.

2) *Non matched transmission line:* We compare here several unmatched cases for the $-\hat{x}$ polarised plane wave from $\theta = \pi/2$, and $\varphi = \pi/2$, shown in Figure 15 for frequency 60 MHz. The matched solutions are given in Eqs. (67) and (68), and for this frequency ($kL = \pi/4$) are:

$$V(z) = 1 - e^{-j\pi/4} \cos(kz) \quad (73)$$

$$Z_0 I(z) = j e^{-j\pi/4} \sin(kz), \quad (74)$$

as shown in Figure 17.

We generalize them for non matched cases using Eqs (49) and (54), obtaining the correction terms due to non matching (Eqs. (50) and (55))

$$\Delta V(z) = \frac{\Gamma_L e^{-jkz} + \Gamma_R e^{jkz} - 2j\Gamma_L \Gamma_R \cos(kz)}{\sqrt{2}(1 + \Gamma_R \Gamma_L)} \quad (75)$$

$$Z_0 \Delta I(z) = \frac{\Gamma_L e^{-jkz} - \Gamma_R e^{jkz} - 2\Gamma_L \Gamma_R \sin(kz)}{\sqrt{2}(1 + \Gamma_R \Gamma_L)} \quad (76)$$

Figures 23-25 show the voltage and normalized current for the cases: $Z_L = Z_0/2$ and $Z_R = 2Z_0$, $Z_L = Z_R = Z_0/2$ and $Z_L = Z_R = 2Z_0$, respectively.

B. Compatibility with previous works

We show in this subsection that our analytic results are compatible with the results obtained by other authors [2]–[6], hence satisfy Eqs. (4) and (5).

Using Eqs. (50), (55) and (56), it is easy to check that

$$\frac{d\Delta V}{dz} + jk(Z_0 \Delta I) = 0 \quad ; \quad Z_0 \frac{d\Delta I}{dz} + jk\Delta V = 0, \quad (77)$$

which is clear, because the induced sources depend only on the incident field and not on the loads.

Therefore, it is enough to show that Eqs. (4) and (5) are satisfied by the matched solution $V(z)$, $I(z)$ in Eqs. (37), (53), for a general incident plane wave.

First we need the phase of the incident plane wave (Eq. (1)) on the TL at $x \simeq 0$, $y = 0$ and $-L \leq z \leq L$, which comes out

$$e^{jkz \cos \theta}, \quad (78)$$

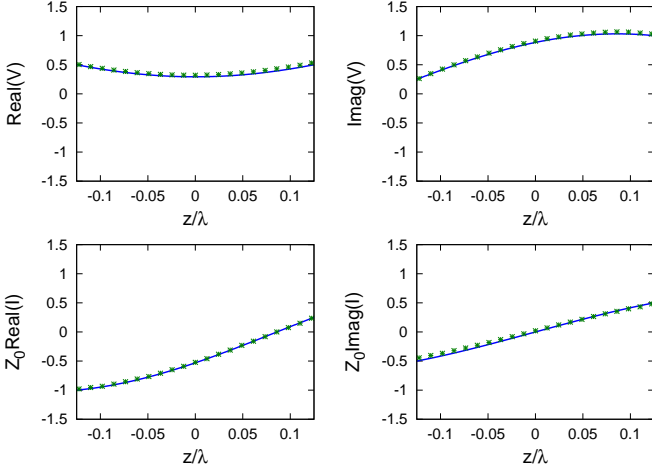


Fig. 23. Real and imaginary parts of the voltage $V(z)$ and normalized current $Z_0I(z)$ for the plane wave incidence shown in Figure 15, at frequency 60MHz (or $L/\lambda = 1/16$), but for loads $Z_L = Z_0/2$ and $Z_R = 2Z_0$, or $\Gamma_L = -1/3$ and $\Gamma_R = 1/3$. The continuous line is the analytic solution, i.e. Eq. (73) plus correction (75) and Eq. (74) plus correction (76) and the stars are the ANSYS simulation results.

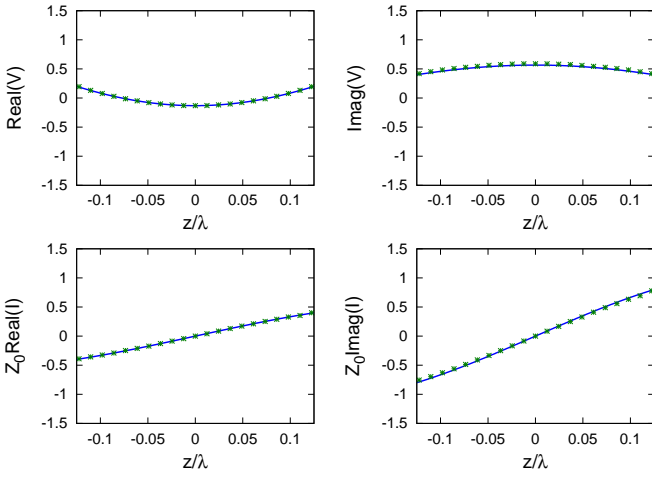


Fig. 24. Same as Figure 23 for $Z_L = Z_R = Z_0/2$ or $\Gamma_L = \Gamma_R = -1/3$.

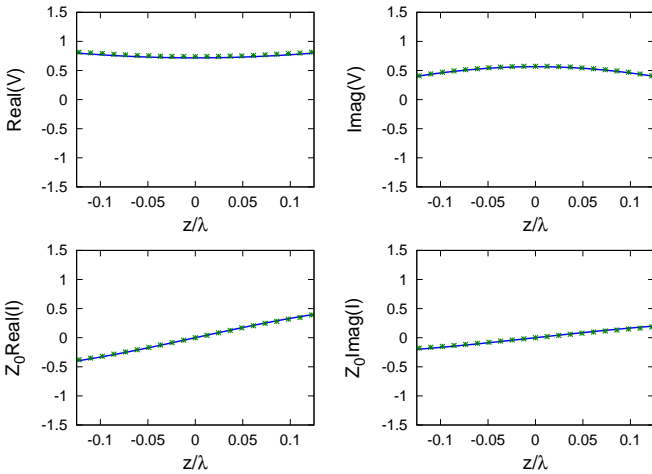


Fig. 25. Same as Figure 23 for $Z_L = Z_R = 2Z_0$ or $\Gamma_L = \Gamma_R = 1/3$.

so the incident E_x and H_y fields along the TL are

$$E_x(z) = E_x e^{jkz \cos \theta} \quad ; \quad H_y(z) = H_y e^{jkz \cos \theta}, \quad (79)$$

where the values E_x and H_y are understood as the values at the origin. Using the unit vectors identity $\hat{\mathbf{x}} = \hat{\mathbf{r}} \sin \theta \cos \varphi + \hat{\boldsymbol{\theta}} \cos \theta \cos \varphi - \hat{\boldsymbol{\phi}} \sin \varphi$, given the incident E field has only θ and φ components, the x component of the electric field (at origin) is

$$E_x = E_\theta \cos \theta \cos \varphi - E_\varphi \sin \varphi = E_0 (\cos \alpha \cos \theta \cos \varphi - \sin \alpha \sin \varphi) \quad (80)$$

where for the second expression we used Eq. (3). Using Eqs. (11), (79) and (80), Z_0I_s in Eq. (7) comes out

$$Z_0I_s = jkV^+ (\sin \alpha \sin \varphi - \cos \alpha \cos \theta \cos \varphi) e^{jkz \cos \theta}, \quad (81)$$

To derive the H_y component of the incident field we note that the H components of the incident plane wave are:

$$H_\theta = \frac{E_\varphi}{\eta_0} \quad ; \quad H_\varphi = -\frac{E_\theta}{\eta_0} \quad (82)$$

Using the unit vectors identity $\hat{\mathbf{y}} = \hat{\mathbf{r}} \sin \theta \sin \varphi + \hat{\boldsymbol{\theta}} \cos \theta \sin \varphi + \hat{\boldsymbol{\phi}} \cos \varphi$, given the incident H field has only θ and φ components, the y component of H (at origin) is

$$H_y = H_\theta \cos \theta \sin \varphi + H_\varphi \cos \varphi = \frac{1}{\eta_0} [E_\varphi \cos \theta \sin \varphi - E_\theta \cos \varphi], \quad (83)$$

where in the second expression we used Eq. (82). Using Eqs. (3) and (11), this can be rewritten as

$$\eta_0 H_y = V^+ [\sin \alpha \cos \theta \sin \varphi - \cos \alpha \cos \varphi], \quad (84)$$

Using Eqs. (79), V_s in Eq. (6) comes out

$$V_s = jkV^+ [\sin \alpha \cos \theta \sin \varphi - \cos \alpha \cos \varphi] e^{jkz \cos \theta}, \quad (85)$$

Here it is left to show that Eqs. (81) and (85) equal to the LHS of Eqs. (5) and (4) respectively, applied on the matched solution $V(z)$, $I(z)$ given in Eqs. (37), (53). We start with two intermediate results for the functions $f_1(z)$ and $f_2(z)$ defined in Eq. (22):

$$\begin{aligned} df_1/dz + jkf_1 &= k \cos^2(\theta/2) e^{jkz \cos \theta} \\ df_2/dz - jkf_2 &= -k \sin^2(\theta/2) e^{jkz \cos \theta}, \end{aligned} \quad (86)$$

and obtain

$$\frac{dV}{dz} + jk(Z_0I) = -jkV^+ [\cos^2(\theta/2) \cos(\varphi + \alpha) + \sin^2(\theta/2) \cos(\varphi - \alpha)] e^{jkz \cos \theta} \quad (87)$$

$$Z_0 \frac{dI}{dz} + jkV = jkV^+ [\sin^2(\theta/2) \cos(\varphi - \alpha) - \cos^2(\theta/2) \cos(\varphi + \alpha)] e^{jkz \cos \theta} \quad (88)$$

Using simple trigonometric identities one finds that results (87) and (88) are identical to Eqs. (85) and (81), respectively.

V. THE POWER TRANSFERRED TO THE LOADS

We calculate here the power transferred to the loads for the general case of loads Z_L and Z_R as shown in Figures 1 and 2. We need first the voltage and current for the *matched at both terminations* case at the terminations ($z = \pm L$). From Eqs. (37) and (53) we obtain

$$V(-L) = jV^+ e^{-jkL} \sin[2kL \sin^2(\theta/2)] \cos(\varphi - \alpha) \quad (89)$$

$$V(L) = -jV^+ e^{-jkL} \sin[2kL \cos^2(\theta/2)] \cos(\varphi + \alpha) \quad (90)$$

and

$$Z_0 I(-L) = -V(-L) \quad ; \quad Z_0 I(L) = V(L) \quad (91)$$

satisfy the boundary conditions. From Eqs. (89)-(91), the powers on the “left” and “right” loads for the *matched at both terminations* case, are

$$P(-L) \equiv -V(-L)I^*(-L) = \frac{|V^+|^2}{Z_0} \sin^2[2kL \sin^2(\theta/2)] \cos^2(\varphi - \alpha) \quad (92)$$

$$P(L) \equiv V(L)I^*(L) = \frac{|V^+|^2}{Z_0} \sin^2[2kL \cos^2(\theta/2)] \cos^2(\varphi + \alpha) \quad (93)$$

We now generalise the powers for a TL with any loads. We set $z = \pm L$ in Eqs. (49), (54), or simpler, use directly Eqs. (47), (48), (C.28) and (C.29), obtaining

$$V_{\text{NM}}(-L) = (1 + \Gamma_L) \frac{\Gamma_R e^{-j2kL} V(L) + V(-L)}{1 - \Gamma_L \Gamma_R e^{-j4kL}} \quad (94)$$

$$V_{\text{NM}}(L) = (1 + \Gamma_R) \frac{\Gamma_L e^{-j2kL} V(-L) + V(L)}{1 - \Gamma_L \Gamma_R e^{-j4kL}} \quad (95)$$

and

$$Z_L I_{\text{NM}}(-L) = -V_{\text{NM}}(-L) \quad ; \quad Z_R I_{\text{NM}}(L) = V_{\text{NM}}(L) \quad (96)$$

satisfy the boundary conditions.

Now we express the power on the “left” load Z_L by $P_{\text{NM}}(-L) = \text{Re}\{-V_{\text{NM}}(-L)I_{\text{NM}}^*(-L)\}$ and on the “right” load Z_R by $P_{\text{NM}}(L) = \text{Re}\{V_{\text{NM}}(L)I_{\text{NM}}^*(L)\}$. Using Eqs. (94)-(96) one obtains

$$P_{\text{NM}}(-L) = \frac{1 - |\Gamma_L|^2}{|1 - \Gamma_L \Gamma_R e^{-j4kL}|^2} [P(-L) + |\Gamma_R|^2 P(L) - 2P_{\text{mix}} \text{Re}\{\Gamma_R e^{-j2kL}\}] \quad (97)$$

$$P_{\text{NM}}(L) = \frac{1 - |\Gamma_R|^2}{|1 - \Gamma_L \Gamma_R e^{-j4kL}|^2} [P(L) + |\Gamma_L|^2 P(-L) - 2P_{\text{mix}} \text{Re}\{\Gamma_L e^{-j2kL}\}]. \quad (98)$$

The generalised results for the powers are expressed in terms of the matched-TL powers $P(-L)$ and $P(L)$ (given in Eqs. (92)-(93)) plus an additional “mixed” term P_{mix} given by

$$P_{\text{mix}} \equiv V(L)I^*(-L) \equiv -V(-L)I^*(L) = \frac{|V^+|^2}{Z_0} \sin[2kL \sin^2(\theta/2)] \sin[2kL \cos^2(\theta/2)] \cos(\varphi - \alpha) \cos(\varphi + \alpha) \quad (99)$$

Those results may be understood from the radiation properties of the TL in [1]. We remark $P(-L)$ is proportional to $\sin^2[2kL \sin^2(\theta/2)]$, according to the radiation pattern of a TL carrying a forward wave only and maximised for the polarisation radiated in this case:

$$\hat{\mathbf{p}}^+(\theta, \varphi) = \hat{\boldsymbol{\theta}} \cos \varphi + \hat{\boldsymbol{\varphi}} \sin \varphi \Rightarrow \alpha = \varphi, \quad (100)$$

see Section 2.1 in [1]. Also, we see $P(-L) = 0$ for a polarisation orthogonal to $\hat{\mathbf{p}}^+$. This suggests that $P(-L)$, i.e. the power into the left load for the matched on both sides TL is closely related to transmitting properties of a source at the left termination, issuing a forward wave.

Similarly, $P(L)$ is proportional to $\sin^2[2kL \cos^2(\theta/2)]$, according to the radiation pattern of a TL carrying a backward wave only and maximised for the polarisation radiated in this case:

$$\hat{\mathbf{p}}^-(\theta, \varphi) = \hat{\boldsymbol{\theta}} \cos \varphi - \hat{\boldsymbol{\varphi}} \sin \varphi \Rightarrow \alpha = -\varphi, \quad (101)$$

see Section 2.2 in [1], and $P(L) = 0$ for a polarisation orthogonal to $\hat{\mathbf{p}}^-$. This suggests that $P(L)$, i.e. the power into the right load for the matched on both sides TL is closely related to transmitting properties of a source at the right termination, issuing a backward wave.

The general non matched case given in Eqs. (97)-(98) is affected by both radiation patterns and polarisations, and their combination found in the mixed term in Eq. (99). We remark that for a polarisation orthogonal to either $\hat{\mathbf{p}}^+$ or $\hat{\mathbf{p}}^-$, $P_{\text{mix}} = 0$ and either $P(-L)$ or $P(L)$ are 0, in which case the received powers are either according to $\sin^2[2kL \cos^2(\theta/2)]$ or $\sin^2[2kL \sin^2(\theta/2)]$.

The formal connection between the transmitting and receiving properties of TL is analysed the next section.

VI. CONSISTENCY BETWEEN TRANSMITTING-RECEIVING RADIATION PROPERTIES

To analyse the connection between the results of receiving electromagnetic radiation shown in this work and the results of transmitting (radiating) electromagnetic radiation in [1], we have to summarise below some results from [1] and rewrite them in a convenient form.

The far electric field radiated by a TL carrying a forward wave only as in the upper panel of Figure 26, is given in

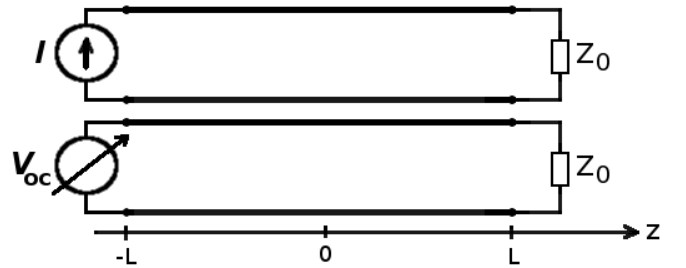


Fig. 26. Upper panel: radiating TL fed by a current source I at $z = -L$, matched at $z = L$. Lower panel: the same TL in receive mode, with a voltmeter at $z = -L$ measuring the open circuit voltage V_{oc} .

Section 2.1 of [1] in terms of the value of I^+ in the middle

of the TL at $z = 0$. We rewrite it here in terms of the current source I in the standard form for a radiating antenna fed by a current

$$\mathbf{E}^+ = jk\eta_0 G(r) \mathbf{I}_{\text{eff}}^+, \quad (102)$$

where $\mathbf{I}_{\text{eff}}^+$ is the effective antenna length for the radiation of a TL carrying a forward wave only, is given by

$$\mathbf{I}_{\text{eff}}^+ = 2j d e^{-jkL} \sin[2kL \sin^2(\theta/2)] \hat{\mathbf{p}}^+ \quad (103)$$

where the polarisation vector $\hat{\mathbf{p}}^+$ is defined in Eq. (100).

The radiation resistance for this case (given in Eq.(36) of [1]) is

$$r_{\text{rad}} = \frac{\eta_0}{2\pi} (kd)^2 [1 - \text{sinc}(4kL)], \quad (104)$$

which does not need a “+” superscript, being valid also for a backward wave only. The radiation pattern (directivity) for a forward wave only is

$$D^+(\theta) = \frac{\eta_0 k^2}{4\pi r_{\text{rad}}} |\mathbf{I}_{\text{eff}}^+|^2 = 2 \frac{\sin^2[2kL \sin^2(\theta/2)]}{[1 - \text{sinc}(4kL)]}, \quad (105)$$

as given in Section 2.1, Eq. (13) in [1]. When dealing with radiation from TL, which is usually small relative to the power carried by the TL, we may use the term “radiation losses” for the power lost to radiation. So in the upper panel of Figure 26, the radiated power is $|I|^2 r_{\text{rad}}$, and the power transmitted by the TL is $|I|^2 Z_0$, and clearly $r_{\text{rad}} \ll Z_0$. But in the context of the radiating properties we have to consider the radiation efficiency, defined as the radiated power, divided by the total power into the antenna. In our case this is

$$e_r = \frac{r_{\text{rad}}}{r_{\text{rad}} + Z_0} \simeq \frac{r_{\text{rad}}}{Z_0}. \quad (106)$$

which is small, meaning that the (matched) TL is not an efficient antenna. Eq. (106) is valid for both forward only or backward only wave, hence does not need a superscript. The antenna gain is the directivity multiplied by the efficiency:

$$G^+(\theta) = D^+(\theta) e_r = \frac{(kd)^2 \eta_0 \sin^2[2kL \sin^2(\theta/2)]}{\pi Z_0}, \quad (107)$$

Now, in receive mode, calculating the scalar product between the incident plane wave (Eq. (2)) and the effective length in Eq. (103) yields the open circuit voltage measured in the lower panel of Figure 26

$$V_{\text{oc}} = \mathbf{E} \cdot \mathbf{I}_{\text{eff}}^+ = 2j E_0 d e^{-jkL} \sin[2kL \sin^2(\theta/2)] \cos(\varphi - \alpha), \quad (108)$$

which is compared with the open end voltage obtained from the formalism developed in this work. So using Eq. (94) with $\Gamma_R = 0$ and $\Gamma_L = 1$ (open) yield exactly the result (108) where we identify $V^+ = E_0 d$ according to Eq. (11). Also, the absolute value of V_{oc} is maximal for a matched polarisation, i.e. for $\alpha = \varphi$.

We replace now the voltmeter in the lower panel of Figure 26 by a load Z_L (left). Eq. (97), reduces for $\Gamma_R = 0$ to $P_{\text{NM}}(-L) = (1 - |\Gamma_L|^2) P(-L)$, so maximum power is obtained for $\Gamma_L = 0$ ($Z_L = Z_0$), yielding Eq. (92). Using the matched polarisation ($\alpha = \varphi$) in (92) results in the maximum received power:

$$P_{\text{rec}} = \frac{|V^+|^2}{Z_0} \sin^2[2kL \sin^2(\theta/2)]. \quad (109)$$

Dividing this by the Poynting vector $S = E_0^2/\eta_0$, results in the effective receiving cross section area A^+ (for receiving into the left termination - the equivalent of transmitting a forward wave)

$$A^+ = \frac{P_{\text{rec}}}{S} = \frac{d^2 \eta_0}{Z_0} \sin^2[2kL \sin^2(\theta/2)]. \quad (110)$$

which equals exactly to $\frac{\lambda^2}{4\pi} G^+$.

A similar analysis for the backward wave, using the current source at the $z = L$ termination (pointing upward) and the matched load at $z = -L$ in Figure 26 yields the field radiated by a backward wave current:

$$\mathbf{E}^- = jk\eta_0 G(r) \mathbf{I}_{\text{eff}}^-, \quad (111)$$

where $\mathbf{I}_{\text{eff}}^-$ is the effective antenna length for the radiation of a TL carrying a backward wave only, is given by

$$\mathbf{I}_{\text{eff}}^- = -2j d e^{-jkL} \sin[2kL \cos^2(\theta/2)] \hat{\mathbf{p}}^-, \quad (112)$$

and the polarisation vector $\hat{\mathbf{p}}^-$ is defined in Eq. (101). For this case, the gain is the directivity function D^- given in Eq. (17) of [1] multiplied by the efficiency in Eq. (106), yields

$$G^-(\theta) = \frac{(kd)^2 \eta_0 \sin^2[2kL \cos^2(\theta/2)]}{\pi Z_0}, \quad (113)$$

The effective receiving cross section area A^- comes out

$$A^- = \frac{d^2 \eta_0}{Z_0} \cos^2[2kL \cos^2(\theta/2)], \quad (114)$$

satisfying the relation $A^- = \frac{\lambda^2}{4\pi} G^-$.

VII. CONCLUSIONS

We derived in this work the voltage and differential current developed on an ideal two-conductors TEM transmission line (TL) of any small electric cross section, connected to passive loads and hit by a monochromatic plane wave, as shown in Figure 1.

For this derivation we used our knowledge on the radiation properties of TL [1] to build S matrices which describe the radiating system and used the reciprocity to derive the current and voltage induced on the TL. This methodology allowed us to derive first the voltage and current on a matched at both terminations TL, yielding the relatively simple expressions given in Eqs. (37) and (53). The generalisation to any loads is then obtained, using the S matrix.

We validated our analytic results in Section IV-A for both the matched on two sides TL case and the non matched case for different plane wave incidences. We also showed in Section IV-B that our analytic results are compatible with the methodology used in previous works [2]–[6]. The simplicity of this proof, requiring the application of Eqs. (4) and (5) *only* on the matched at both terminations solution (see Eq. 77), emphasises the added value of this work.

In Section V, we derived the powers on the loads and showed the connection between those powers and the radiating properties of the TL. For the matched at both terminations TL, the power on the “left” load has the same spatial dependence on the incident plane wave direction as the radiation pattern

of a forward wave, and is maximised for the polarisation of a radiating forward wave $\hat{\mathbf{p}}^+$ (see Eq. (100)). Similarly, for the matched at both terminations TL, the power on the “right” load has the same spatial dependence on the incident plane wave direction as the radiation pattern of a backward wave, and is maximised for the polarisation $\hat{\mathbf{p}}^-$ (see Eq. (101)). The general non matched case is affected by both radiation patterns and polarisations, and their combination found in a mixed term.

In Section VI we showed that the formal relations between receiving cross section area and antenna gain are satisfied for the TL.

APPENDIX A

FAR RADIATED E FIELD AND ITS NORMALIZATION

To derive the S matrices we need the contribution of currents shown in Figure A.1 to the far field. Based on [1], a current element $I d$ in the x direction (where I is the current and d the separation distance in the twin lead representation), at $z = z_w$ (w =wire) contributes the following E field in θ and φ polarisations (see left panel of Figure A.1).

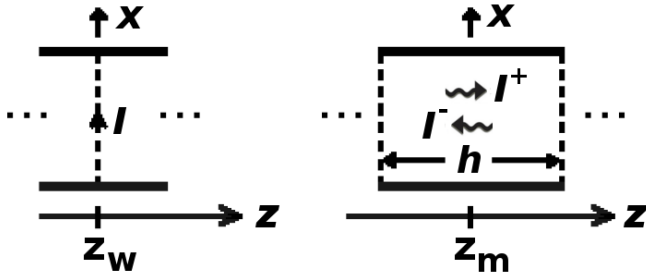


Fig. A.1. Currents contributing to radiation. The left panel shows a x directed current I at location z_w on the TL (which may represent a parallel port or a load), contributes to the far E field according to Eqs. (A.1) and (A.2). The right panel shows a TL segment of width h carrying a forward and/or backward current wave, I^\pm evaluated at the middle location z_m , contributing to the far E field according to Eq. (A.3).

$$E_{\theta(x)} = -jkG(r)\eta_0 dI e^{jkz_w \cos \theta} \cos \theta \cos \varphi \quad (\text{A.1})$$

$$E_{\varphi(x)} = jkG(r)\eta_0 dI e^{jkz_w \cos \theta} \sin \varphi, \quad (\text{A.2})$$

where the subscript (x) shows that this is a x directed current contribution.

A TL section of length h around $z = z_m$ (m =middle) carrying a forward and/or backward current contributes the following far θ polarised E fields (see right panel of Figure A.1).

$$E_{\theta(z)} = -2kG(r)\eta_0 dI^\pm(z_m) e^{jkz_m \cos \theta} (1 \pm \cos \theta) \cos \varphi \sin[kh(1 \mp \cos \theta)/2] \quad (\text{A.3})$$

where the upper and lower signs are for forward and backward waves respectively, and the values used for the forward or backward currents are in the middle of the line at z_m , both currents defined in the $+z$ direction. The subscript (z) shows that this is a z directed current contribution.

In the final result, $E_\theta = E_{\theta(x)} + E_{\theta(z)}$ and $E_\varphi = E_{\varphi(x)}$. To work out the S matrices (Section II and Appendix C), one needs to scale the radiated E_θ and E_φ fields to outgoing

voltages V_θ^- and V_φ^- at the ports θ and φ (Section II), or to outgoing currents I_θ^- and I_φ^- (Appendix C). Those ports have been defined for the impedance Z_0 , which is the characteristic impedance of the analysed TL. To make those ports matched, we use the antenna model shown in Figure A.2. The model assumes a real antenna impedance Z_A matched

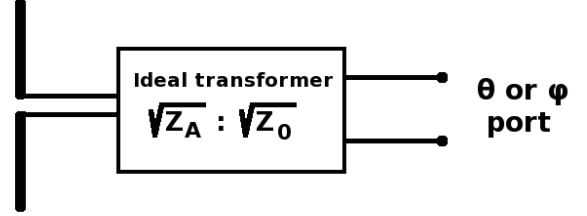


Fig. A.2. The antenna model assumes a real antenna impedance Z_A matched by an ideal transformer to the θ or φ port of impedance Z_0 .

via an ideal transformer to the θ or φ port of impedance Z_0 . Using the effective length of the antenna l_{eff} (for the given incidence direction), one expresses the open circuit voltage on the antenna [9]

$$V_{\text{oc}} = E l_{\text{eff}}, \quad (\text{A.4})$$

where E is E_θ or E_φ . The θ or φ port being matched, the antenna “sees” a matched load, so that the actual voltage on the antenna terminals is $V_{\text{oc}}/2$, and the outgoing voltage at the port is

$$V^- = \frac{1}{2} E l_{\text{eff}} \sqrt{Z_0/Z_A}. \quad (\text{A.5})$$

Now to activate the antenna in transmit mode, we feed the θ or φ port by V^+ , obtaining the current feeding the antenna

$$I_A = V_A/Z_A = V^+/\sqrt{Z_A Z_0} \quad (\text{A.6})$$

Using the well known formula for the far E field radiated by a dipole [9]

$$E_0 = jk\eta_0 G(r) I_A l_{\text{eff}} \quad (\text{A.7})$$

where l_{eff} is the effective dipole length discussed before, into the same direction [9]. The field radiated from the antenna(s) has been named E_0 to distinguish it from the previously discussed field travelling toward the antenna(s). Expressing it as function of V^+ , we obtain

$$E_0 = jk\eta_0 G(r) l_{\text{eff}} V^+ / \sqrt{Z_A Z_0} \quad (\text{A.8})$$

This field E_0 radiated from the far antenna(s), is the field incident on the TL (or one of its components), mentioned in Figure 3. We want to normalise it so that $E_0 d = V^+$ (see Eq. (11)), considering the field incident on the TL as a plane wave. Imposing condition (11) on Eq. (A.8), results in

$$l_{\text{eff}} = \frac{\sqrt{Z_A Z_0}}{jk\eta_0 G(r) d} \quad (\text{A.9})$$

Given the far antennas are only tools to build the S matrices and from them infer the voltage and current along the TL, the “actual” value of l_{eff} is of no interest, so to express the fields

radiated by the TL E_θ and E_φ as voltages, we set l_{eff} from (A.9) into Eq. (A.5), obtaining

$$V_{\theta \text{ or } \varphi}^- = \frac{Z_0 E_{\theta \text{ or } \varphi}}{2jk\eta_0 G(r)d} \quad (\text{A.10})$$

For the case we need to express the fields radiated by the TL E_θ and E_φ as outgoing currents (Section C), we use $I^- = -V^-/Z_0$, obtaining:

$$I_{\theta \text{ or } \varphi}^- = -\frac{E_{\theta \text{ or } \varphi}}{2jk\eta_0 G(r)d} \quad (\text{A.11})$$

APPENDIX B GENERALISED SCATTERING MATRIX

In this appendix we define the generalized scattering matrix and explain its reciprocity properties. The generalized scattering matrix [7] for an arbitrary network (as shown in Figure B.1) is defined by the following matrix equation

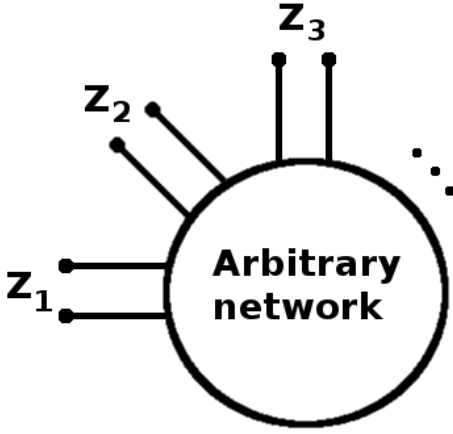


Fig. B.1. An N ports arbitrary network interfaced to transmission lines of characteristic impedances Z_1, Z_2, \dots, Z_N .

$$\mathbf{V}^- = \mathbf{S}\mathbf{V}^+, \quad (\text{B.1})$$

where \mathbf{V}^\pm are column vectors for the incoming and outgoing voltage waves at the ports of the network, where each port has its own characteristic impedance, as shown in Figure B.1. The voltage and current waves at the ports satisfy

$$\mathbf{V}^+ = \mathbf{Z}\mathbf{I}^+ ; \quad \mathbf{V}^- = -\mathbf{Z}\mathbf{I}^-, \quad (\text{B.2})$$

where \mathbf{Z} is a diagonal matrix of the characteristic impedances in Figure B.1:

$$Z_{ij} = Z_i \delta_{ij}, \quad (\text{B.3})$$

so one can easily apply functions on them, as follows.

Normalising the voltages and currents at each port according to

$$\mathbf{a}^\pm \equiv \sqrt{\mathbf{Z}^{-1}}\mathbf{V}^\pm ; \quad \mathbf{b}^\pm \equiv \sqrt{\mathbf{Z}}\mathbf{I}^\pm, \quad (\text{B.4})$$

and setting into Eq. (B.1), result in

$$\mathbf{a}^- = \sqrt{\mathbf{Z}^{-1}}\mathbf{S}\sqrt{\mathbf{Z}}\mathbf{a}^+, \quad (\text{B.5})$$

which define the (ordinary) scattering matrix, for which we use a lower case “s”

$$\mathbf{s} \equiv \sqrt{\mathbf{Z}^{-1}}\mathbf{S}\sqrt{\mathbf{Z}}. \quad (\text{B.6})$$

It is known [7]–[12] that the reciprocity condition for the ordinary scattering matrix is

$$s_{ij} = s_{ji}. \quad (\text{B.7})$$

Using this in Eq. (B.6) results in the reciprocity condition for the generalized scattering matrix

$$S_{ij}Z_j = S_{ji}Z_i \quad (\text{B.8})$$

Scattering matrices are usually defined for voltage waves, but in this work we need to define a generalized scattering matrix for current waves as follows

$$\mathbf{I}^- = \mathbf{S}_I\mathbf{I}^+, \quad (\text{B.9})$$

and we name it \mathbf{S}_I to distinguish it from the regular scattering matrix in (B.1). Using Eq. (B.2), one obtains

$$\mathbf{V}^- = -\mathbf{Z}\mathbf{S}_I\mathbf{Z}^{-1}\mathbf{V}^+. \quad (\text{B.10})$$

Comparing it with (B.1) we get the relation

$$\mathbf{S} = -\mathbf{Z}\mathbf{S}_I\mathbf{Z}^{-1}. \quad (\text{B.11})$$

Setting it in (B.6) results in

$$\mathbf{s} = -\sqrt{\mathbf{Z}}\mathbf{S}\sqrt{\mathbf{Z}^{-1}}, \quad (\text{B.12})$$

and using (B.7) we obtain

$$S_{Iij}Z_i = S_{Iji}Z_j \quad (\text{B.13})$$

APPENDIX C DERIVATION OF THE CURRENT ALONG THE TL

We define a system of $M + 2$ ports, the first M ports are serial ports on the TL (shown in Figure 6) and 2 additional ports are far antennas at polarisations $\hat{\theta}$ and $\hat{\varphi}$.

Our purpose is to determine the TL current for an incidence of a plane wave, we therefore calculate the matrix S defined by

$$\mathbf{I}^- = \mathbf{S}\mathbf{I}^+, \quad (\text{C.1})$$

although this is not the usual definition of the scattering matrix (see Appendix B). For simplicity, we still call it S , but take into consideration that any reflection coefficient has an opposite sign.

Feeding port $1 < n < M$, located at z_n with a forward (entering) current I_n^+ and terminating the other TL ports $1 \leq i \leq M$ by the impedances defined for those ports (i.e. Z_0 for ports 1 and M , and Z_T for the middle ports) results in a forward wave from $z = z_n$ to $z = L$ and a backward wave from $z = z_n$ to $z = -L$, because the waves encounter at the intermediate ports a very small serial impedance $Z_T \rightarrow 0$.

The reflection coefficient at port n is $S_{n,n} = \frac{Z_T - 2Z_0}{Z_T + 2Z_0} \simeq -1 + \frac{Z_T}{Z_0}$, so the port current $I_n = I_n^+(1 + S_{nn}) \simeq I_n^+ \frac{Z_T}{Z_0}$. The current waves at ports $i \neq n$ give rise to outgoing currents at the ports given by:

$$I_{i \neq n}^- = I_n e^{-jk\Delta z|i-n|} = I_n^+ \frac{Z_T}{Z_0} e^{-jk\Delta z|i-n|}. \quad (\text{C.2})$$

and for $i = n$

$$I_n^- = I_n^+ S_{n,n} = I_n^+ \left(-1 + \frac{Z_T}{Z_0} \right) \quad (\text{C.3})$$

This results in the following (partial) n column of the S matrix

$$S_{1 \leq i \leq M, 1 < n < M} = \begin{cases} \frac{Z_T}{Z_0} e^{-jk\Delta z |i-n|} & i \neq n \\ -1 + \frac{Z_T}{Z_0} \simeq -1 & i = n \end{cases}, \quad (\text{C.4})$$

see lower sign in Figure 5. For column $n = 1$ or M , the results are similar, only replace $\frac{Z_T}{Z_0}$ by 1, hence

$$S_{1 \leq i \leq M, n=1, M} = \begin{cases} e^{-jk\Delta z |i-n|} & i \neq n \\ 0 & i = n \end{cases} \quad (\text{C.5})$$

Eqs. (C.4) and (C.5) define the upper left square of the S matrix, i.e. all the elements connecting the TL ports 1 to M , and now we calculate the two additional elements belonging to ports θ and φ (last two columns in Figure 5), using Eqs. (A.1)-(A.3) and scaling the fields with Eq. (A.11).

Feeding a *middle* port $1 < n < M$ with the current I_n^+ and terminating all other ports with matched loads, we calculate the far fields given in Eqs. (A.1)-(A.3), scaled to the currents I_θ^- and I_φ^- according to Eq. (A.11). As in the voltage calculation section, the value of n is hidden in the parameters l_1 and l_2 (Eq. (21)), see Figure C.1.

We start with the contribution of the x currents given in Eqs. (A.1) and (A.2). The x directed currents are shown in Figure C.1. Using Eqs.(A.1) for the two currents at L and

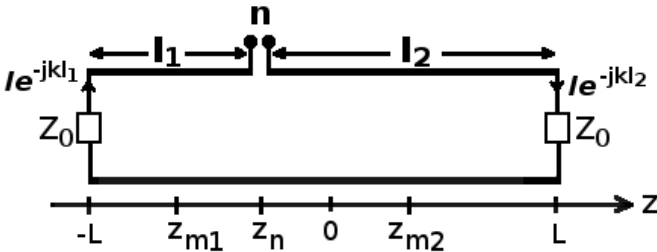


Fig. C.1. Currents in the TL while feeding port n with I_n^+ . Defining $I \equiv I_n^+ Z_T / Z_0$, the x directed currents are $I e^{-jk l_1}$ in port 1 at $z = -L$ and $-I e^{-jk l_2}$ in port M at $z = L$. The z directed current waves are the forward wave in the region $[z_n, L]$ and the backward current wave in the region $[-L, z_n]$, to be used in Eq. (A.3). For the forward wave we use the current at the middle point $z_{m2} = (z_n + L)/2$, which is $I e^{-jk l_2 / 2}$, while for the backward wave we use the current at $z_{m1} = (z_n - L)/2$ which is $I e^{-jk l_1 / 2}$.

$-L$, scaling with (A.11), we obtain after some algebra:

$$I_{\theta(x)}^- = j I_n^+ (Z_T / Z_0) [f_2 - f_1] \cos \theta \cos \varphi, \quad (\text{C.6})$$

where $f_{1,2}$ are defined in Eq. (22). As evident from Eqs.(A.1) and (A.2), $I_{\varphi(x)}^-$ is identical to the above, up to replacing $\cos \theta \cos \varphi$ by $-\sin \varphi$, we therefore have

$$I_{\varphi(x)}^- = j I_n^+ (Z_T / Z_0) [f_1 - f_2] \sin \varphi \quad (\text{C.7})$$

Next we calculate the contributions of the forward current wave in the region $z = [z_n, L]$ and the backward current wave in the region $z = [-L, z_n]$ (see Figure C.1), using the upper and lower signs in Eq. (A.3), respectively. For the forward

wave we use the current in the middle point z_{m2} , having the phase $e^{-jk l_2 / 2}$ for a TL length $h = l_2$, while for the backward wave we use the current at z_{m1} , having the phase $e^{-jk l_1 / 2}$, for a TL length $h = l_1$, both currents are defined in the $+z$ direction, hence taken with plus sign. Using $z_{m1,2}$ in Eq. (25), after scaling with (A.11), we obtain:

$$I_{\theta(z)}^- = -2j I_n^+ (Z_T / Z_0) [f_2 \cos^2(\theta/2) + f_1 \sin^2(\theta/2)] \cos \varphi \quad (\text{C.8})$$

Now we add the x and z directed currents contributions to $I_\theta^- = I_{\theta(x)}^- + I_{\theta(z)}^-$, using $1 - \cos(\theta) = 2 \sin^2(\theta/2)$ and $1 + \cos(\theta) = 2 \cos^2(\theta/2)$, after some algebra we obtain:

$$I_\theta^- = -j I_n^+ (Z_T / Z_0) [f_1 + f_2] \cos \varphi \quad (\text{C.9})$$

I_φ^- has only the contribution of the x directed currents, given in Eq (C.7), so that

$$I_\varphi^- = I_{\varphi(x)}^- \quad (\text{C.10})$$

Results (C.9) and (C.10) define the $S_{\theta,n}$ and $S_{\varphi,n}$ matrix elements respectively, for the columns $1 < n < M$:

$$S_{\theta, 1 < n < M} = -j (Z_T / Z_0) [f_1 + f_2] \cos \varphi \quad (\text{C.11})$$

$$S_{\varphi, 1 < n < M} = j (Z_T / Z_0) [f_1 - f_2] \sin \varphi \quad (\text{C.12})$$

For column $n = 1$ or M , the results are similar, only replace $\frac{Z_T}{Z_0}$ by 1, hence

$$S_{\theta, n=1, M} = -j [f_1 + f_2] \cos \varphi \quad (\text{C.13})$$

$$S_{\varphi, n=1, M} = j [f_1 - f_2] \sin \varphi \quad (\text{C.14})$$

The transpose elements are found by the reciprocity condition $S_{i,j} Z_i = S_{j,i} Z_j$ (see Appendix B, Eq. B.13), where Z_i and Z_j are the impedances for which ports i and j have been defined, respectively. Note that this reciprocity condition is different from the one used for the voltage calculation in Section II (see Appendix B).

Given the ports $1, M, \theta$ and φ are defined for Z_0 of the TL and ports $2 \dots M - 1$ are defined for Z_T , the transposed relations $S_{n,\theta}$ and $S_{n,\varphi}$ are given by Eqs. (C.13) and (C.14), for all n :

$$S_{n,\theta} = -j [f_1 + f_2] \cos \varphi \quad (\text{C.15})$$

$$S_{n,\varphi} = j [f_1 - f_2] \sin \varphi \quad (\text{C.16})$$

When issuing an excitation I_θ^+ from the θ port and matching all other ports, the currents at ports n on the TL are $I_n^- = I_\theta^+ S_{n,\theta}$. Given the number M is not limited, one can get the continuous current on the TL for the excitation of the θ port:

$$I_\theta(z) = -j I_\theta^+ [f_1(z) + f_2(z)] \cos \varphi \quad (\text{C.17})$$

and similarly for the φ port:

$$I_\varphi(z) = j I_\varphi^+ [f_1(z) - f_2(z)] \sin \varphi \quad (\text{C.18})$$

where the z dependence in $f_{1,2}$ (see Eq. (22)) is in l_1 and l_2 , defined according to Eq. (21), using z for z_n .

Expressing those in terms of $V_\theta^+ = Z_0 I_\theta^+$, and $V_\varphi^+ = Z_0 I_\varphi^+$ results in Eqs. (51) and (52) in the main text.

The total current developed on the TL is

$$I(z) = I_\theta(z) + I_\varphi(z) \quad (\text{C.19})$$

This concludes the results on a TL matched on both ends. We generalize the above results for TL terminated with any loads at ports 1 and M : Z_L (left) and Z_R (right), respectively. We express the generalized results in terms of the reflection coefficients Γ_L and Γ_R , given in Eqs. (38). For currents they are used with the minus sign.

At ports 1 and M we have:

$$I_1^+ = -\Gamma_L I_1^- \text{ and } I_M^+ = -\Gamma_R I_M^-, \quad (\text{C.20})$$

and at ports $n = 2..M$ (matched with Z_T),

$$I_{2 \leq n \leq M-1}^+ = 0. \quad (\text{C.21})$$

We use the general connection for $1 \leq n \leq M$ (i.e. on TL) but $1 \leq i \leq M+2$, i.e. all excitations including θ and φ :

$$I_n^- = \sum_{i=1}^{M+2} S_{n,i} I_i^+ = S_{n,1} I_1^+ + S_{n,M} I_M^+ + I(z) = -S_{n,1} \Gamma_L I_1^- - S_{n,M} \Gamma_R I_M^- + I(z) \quad (\text{C.22})$$

where the only non zero terms are $i = 1, M, \theta$ and φ (see Eq (C.21)), and the last two terms $i = \theta, \varphi$ represent the matched currents at $z = z_n$, given in (C.17), (C.18), summed in (C.19). In the last form of Eq. (C.22), we used (C.20).

For $n = 1$, Eq. (C.22) becomes

$$I_1^- = -\Gamma_R I_M^- e^{-jk2L} + I(-L). \quad (\text{C.23})$$

because $S_{1,1} = 0$, $S_{1,M} = S_{M,1} = e^{-jk2L}$ and $z_n = -L$.

For $n = M$, Eq. (C.22) reads

$$I_M^- = -\Gamma_L I_1^- e^{-jk2L} + I(L). \quad (\text{C.24})$$

because $S_{M,M} = 0$ and $z_n = L$.

Using $S_{n,1} = e^{-jkl_1}$, $S_{n,M} = e^{-jkl_2}$, for $2 \leq n \leq M-1$, Eq. (C.22) becomes

$$I_{2 \leq n \leq M-1}^- = -e^{-jkl_1} \Gamma_L I_1^- - e^{-jkl_2} \Gamma_R I_M^- + I(z), \quad (\text{C.25})$$

where in principle $I(z)$ here excludes the terminations, but as we shall see this exclusion is not necessary.

We solve now Eqs. (C.23) and (C.24) for I_1^- and I_M^- and obtain:

$$I_1^- = \frac{-\Gamma_R e^{-j2kL} I(L) + I(-L)}{1 - \Gamma_L \Gamma_R e^{-j4kL}} \quad (\text{C.26})$$

$$I_M^- = \frac{-\Gamma_L e^{-j2kL} I(-L) + I(L)}{1 - \Gamma_L \Gamma_R e^{-j4kL}}. \quad (\text{C.27})$$

We need the total (non matched) current $I_{NM}(z_n) = I_n^+ + I_n^-$ for ports 1 to M on the TL, i.e. the outgoing I^- plus the incoming I^+ . For ports 1 or M , this current is

$$I_{NM}(-L) = I_1^-(1 - \Gamma_L) \quad (\text{C.28})$$

$$I_{NM}(L) = I_M^-(1 - \Gamma_R). \quad (\text{C.29})$$

For the ports $2 \leq n \leq M-1$, $I_n^+ = 0$ (C.21), therefore Eq. (C.25) describes the total current on those ports. Taking the limit $z \rightarrow -L$ of Eq. (C.25), using (C.23) we find it reduces to (C.28) and similarly the limit $z \rightarrow L$ of Eq. (C.25) reduces to (C.29), therefore Eq. (C.25) describes the non matched voltage on the TL at all ports (in the continuum, for all z). Hence, $I_{NM}(z) = I(z) + \Delta I(z)$, where $\Delta I(z)$ is the correction term due to non matching:

$$\Delta I(z) = -e^{-jkl_1} \Gamma_L I_1^- - e^{-jkl_2} \Gamma_R I_M^-, \quad (\text{C.30})$$

and I_1^- and I_M^- are given in Eqs. (C.26) and (C.27).

REFERENCES

- [1] Iaconescu, R. and Vulfin, V., "Radiation from free space TEM transmission lines", IET MICROW ANTENNA P (2019)
- [2] Taylor, C., Satterwhite, R., Harrison, C.: "The response of a terminated two-wire transmission line excited by a nonuniform electromagnetic field." IEEE Transactions on Antennas and Propagation 13 (1965): 987-989.
- [3] Smith, A.A., "A More Convenient Form of the Equations for the Response of a Transmission Line Excited by Nonuniform Fields", IEEE transactions on Electromagnetic Compatibility 3 (1973): 151-152
- [4] Harrison, C. W., "Generalized Theory of Impedance Loaded Multiconductor Transmission Lines in an Incident Field", IEEE Transactions on Electromagnetic compatibility 2 (1972): 56-63.
- [5] Paul, C. R.: "Frequency response of multiconductor transmission lines illuminated by an electromagnetic field", IEEE Transactions on Electromagnetic Compatibility 4 (1976): 183-190.
- [6] Agrawal, A.K., Price, H.J., Gurbaxani, S.H.: "Transient response of multiconductor transmission lines excited by a nonuniform electromagnetic field", IEEE Transactions on electromagnetic compatibility 2 (1980): 119-129.
- [7] D. M. Pozar, *Microwave Engineering*, Wiley India Pvt., 2009
- [8] Collin, Robert E. *Antennas and radiowave propagation*, McGraw-Hill, 1985.
- [9] Orfanidis S.J., *Electromagnetic Waves and Antennas*, ISBN: 0130938556, (Rutgers University, 2002)
- [10] S. Ramo, J. R. Whinnery and T. Van Duzer, *Fields and Waves in Communication Electronics*, 3rd edition, Wiley 1994
- [11] E. C. Jordan and K. G. Balmain, *Electromagnetic Waves and Radiating Systems*, 2nd edition, Prentice Hall 1968
- [12] C. A. Balanis, *Antenna Theory: Analysis and Design*, 3rd edition, John Wiley & Sons, 2005